

# From Layers to Submodules: Rethinking Granularity in Replacement-Based LLM Compression

Elia Cunegatti   Marcus Vukojevic   Erik Nielsen   Giovanni Iacca

University of Trento

{elia.cunegatti, marcus.vukojevic, erik.nielsen, giovanni.iacca}@unitn.it

## Abstract

Post-training compression of Large Language Models (LLMs) removes entire architectural components, either deleting them or replacing them with fitted modules. Existing replacement-based methods share two design constraints: full-layer granularity and contiguous selection. We argue that this is overly restrictive: in fact, redundancy in pretrained transformers is not confined to contiguous regions, nor does it evenly distribute between Attention and FeedForward outputs, implying that different strategies best approximate different submodule types and that removable components need not cluster within contiguous depth ranges. Based on this intuition, we introduce SUBFIT (Submodule-level Fitted residual replacement), which compresses LLMs at the *submodule* level: Attention and FeedForward submodules are selected non-contiguously, and each receives its own lightweight fitted residual bypass. SUBFIT operates post-training and requires only calibration data. Across ten LLMs (five base, five instruction-tuned), five sparsity levels from 12.5% to 37.5%, and four replacement-based baselines, SUBFIT achieves the best aggregate perplexity–accuracy trade-off across the evaluated sparsity levels, with larger gains under aggressive compression. At 25% sparsity, it retains 84.6% of dense downstream accuracy and incurs  $2.42\times$  perplexity degradation, against 81.6% and  $4.34\times$  for the strongest baselines, while delivering measurable inference speedup and KV-cache savings. Code is available at <https://github.com/eliacunegatti/SubFit>.

## 1 Introduction

Post-training compression is an established approach to deploying Large Language Models (LLMs) under tight memory and latency constraints (Lin et al., 2024; Xiao et al., 2023). Methods that remove entire architectural components (Ma et al., 2023; Ashkboos et al., 2024) are particularly effective because they yield real infer-

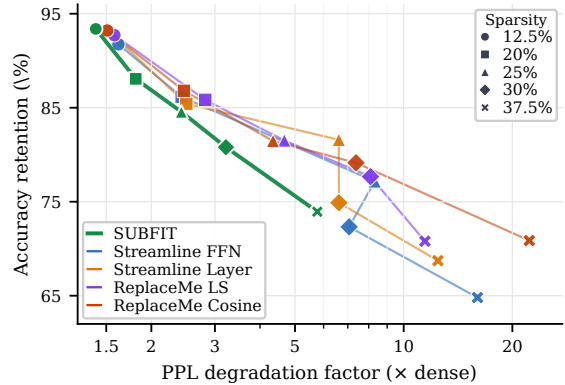


Figure 1: Downstream accuracy retention versus aggregate perplexity degradation across sparsity levels for SUBFIT and four replacement-based baselines.

ence savings without depending on sparse kernels or custom hardware. However, the challenge is that removing components from a pretrained model disrupts the residual stream, and naïve deletion typically incurs sharp quality loss.

A recent line of work addresses this by replacing removed components with lightweight fitted modules or recovery mechanisms (Chen et al., 2025b; Shopkhoev et al., 2025; Liu et al., 2025a; Chen et al., 2026a; Jiang et al., 2026). While these approaches differ in whether they use calibration data, fold the replacement into existing weights, or apply activation correction at inference time, they share the same core observation: recovery after component removal is crucial. However, most operate at the granularity of full layers or contiguous blocks, treating the Transformer layer as the atomic unit of removal. In this work, we frame replacement as a finer-grained alternative to deletion: the goal is not only to remove components, but to identify components whose residual contribution can be approximated efficiently. Attentions require only a low-rank bypass, while FeedForwards (FFNs) need a higher-rank map whose input basis is shared across selected layers to limit deployed cost.

Based on these intuitions, we introduce SUBFIT (Submodule-level Fitted residual replacement), a replacement method that acts at the Attention and FFN submodule-level, selecting components across depths and fitting a residual bypass for each removed submodule.

We evaluate the method on five base LLMs, five instruction-tuned variants, and five sparsity levels from 12.5% to 37.5%, against four post-training, calibration-only replacement baselines from the LLM-Streamline (Chen et al., 2025b) and ReplaceMe (Shopkoev et al., 2025) families. At the aggregate level, i.e., averaging PPL degradation over base models and accuracy retention over instruction-tuned models, SUBFIT achieves the strongest perplexity–accuracy trade-off across the evaluated sparsity levels (Figure 1), with larger gains under aggressive compression: the PPL gap over the strongest baseline grows from  $0.11\times$  at 12.5% to  $1.92\times$  at 25% and  $5.69\times$  at 37.5%, while also obtaining the most stable results. The same pattern holds for downstream accuracy retention on instruction-tuned models, where SUBFIT is the only method among the baselines to retain above 80% at 25% sparsity and above 73% at 37.5%.

To summarize, our contributions are as follows.

(1) We identify two design constraints shared by existing replacement-based compression methods, namely full-layer granularity and contiguous selection. (2) We propose SUBFIT, which selects replaceable Attention and FFN submodules and fits a residual bypass for each, using a shared low-rank basis across FFNs to limit deployed cost. (3) We evaluate SUBFIT on ten LLMs and five sparsity levels, reporting perplexity, downstream accuracy, deployed cost, and inference speedup; results show improved aggregate quality–efficiency trade-offs under increasing compression.

## 2 Related Work

**Post-training LLM compression.** Post-training compression reduces the deployment cost of pre-trained LLMs without requiring retraining. *Quantization* methods reduce the numerical precision of weights, exploiting second-order information (Frantar et al., 2022; Kim et al., 2024) as well as activation statistics (Lin et al., 2024). Other approaches jointly compress weights and activations, improving throughput through outlier-aware corrections (Xiao et al., 2023; Shao et al., 2024). On the other hand, *unstructured pruning*

approaches, such as SparseGPT (Frantar and Alishtarh, 2023) and Wanda (Sun et al., 2024), directly remove weights from the model matrices. However, weight removal often requires sparse kernels or hardware support to translate into a practical runtime speedup. For deployable compression, *structured pruning* is often preferred because it removes entire architectural units, such as rows or columns of a weight matrix (Ashkboos et al., 2024; An et al., 2024), or complete components such as Transformer blocks (Yang et al., 2024; Gromov et al., 2025; Men et al., 2025), Attention heads (Ma et al., 2023), and submodules thereof (Zhong et al., 2025; Sandri et al., 2025). All these methods remove components without replacement. SUBFIT follows the same deployable-compression motivation, but fits a dedicated residual bypass for each removed submodule instead of deleting it outright.

**Compression during training.** Another family of compression approaches relies on jointly compressing and training. Depending on the method, this can involve layer sharing (Xia et al., 2024), sparsity-aware training (Liu et al., 2025b; Tang et al., 2025), or quantization-aware training (Liu et al., 2024; Chen et al., 2025a). These approaches let the model adapt to the compressed structure during optimization, but require additional training resources and runtime, differently from SUBFIT.

**Block replacement and post-pruning recovery.** Replacement-based methods are a recent direction in post-training compression, where the key observation is that recovering the contribution of removed components can improve task performance without full-model fine-tuning and without re-introducing the original parameters. These methods remove Transformer blocks or layers and replace them with lightweight alternatives fitted on calibration data: a small feed-forward module (Chen et al., 2025b), a linear transformation that can be absorbed into adjacent weights (Shopkoev et al., 2025), SVD (Liu et al., 2025a), or a lightweight fixed-point module selected by a learned policy (Jiang et al., 2026). LinearPatch (Chen et al., 2026a) instead targets already layer-pruned models by correcting activation-magnitude mismatch through a linear patch between the remaining blocks. These methods show that recovery after component removal is crucial, but they primarily operate at the granularity of full layers or contiguous blocks. SUBFIT instead performs joint selection and replacement at the Attention and FFN submodule-level, selecting compo-

nents across non-contiguous depths.

### 3 Methodology

SUBFIT compresses pretrained decoder-only Transformer architectures through a two-stage *select-and-replace* procedure. Given a target sparsity  $s$  and a model with  $L$  layers, SUBFIT selects  $\text{round}(Ls)$  Attention submodules and  $\text{round}(Ls)$  FFN submodules independently across depths, and replaces their residual contributions with lightweight fitted bypasses. Selection is non-contiguous: each selected module is chosen independently by score, with no restriction that selected layers form a consecutive block. Figure 2 shows the workflow of SUBFIT.

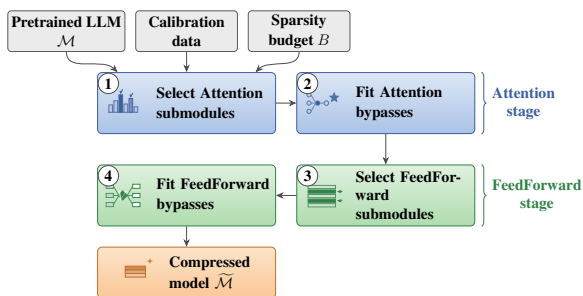


Figure 2: Workflow of SUBFIT. The blue boxes are relative to the Attention submodules replacement, while the green ones are about the FeedForward submodules.

**Notation.** For a submodule  $F_\ell$  at layer  $\ell$ , either Attention or FFN, we denote by  $x \in \mathbb{R}^d$  a generic token-level input and by  $y = F_\ell(x) \in \mathbb{R}^d$  the corresponding residual contribution to be approximated, where  $d$  is the hidden dimension, shared by both input and output of each submodule. Calibration samples are written  $(x_i, y_i)_{i=1}^N$  with  $y_i = F_\ell(x_i)$ , where  $N$  is the number of calibration tokens, and we collect them into matrices  $X_\ell, Y_\ell \in \mathbb{R}^{N \times d}$  to generate our dataset for the fitting stage. The sets of selected Attention and FFN layers are denoted by  $\mathcal{S}_{\text{attn}}$  and  $\mathcal{S}_{\text{fn}}$ , respectively.

**Sequential component selection.** SUBFIT scores and replaces Attention submodules first, then scores FFN submodules on the partially compressed model. This order reflects two properties of pretrained Transformers: Attention submodules tend to be more redundant than FFN submodules (He et al., 2024; Siddiqui et al., 2024), and scoring the second component on post-replacement activations lets FFN selection account for the residual-stream shift induced by Attention replacement, as in activation-driven post-training compression (Frantar and Alistarh, 2023; Sun et al., 2024;

Ashkboos et al., 2024). For Attention, we rank submodules by an *Impact* score computed on calibration activations. Given a residual reference  $h$  and a module contribution  $\delta$ , the per-token score is

$$I(h, \delta) = (1 - \cos(h, h + \delta)) \frac{\|\delta\|_2}{\|h\|_2 + \epsilon}, \quad (1)$$

where  $\epsilon > 0$  is a small constant for numerical stability. The first factor measures how much the submodule rotates the residual stream, as in (Gromov et al., 2025; Chen et al., 2025b), where small values indicate near-identity behavior, consistent with the near-linear per-layer transitions reported for Transformer decoders (Razzhigaev et al., 2024; Shopkhoev et al., 2025). The second factor measures the relative magnitude of the contribution  $\delta$  (He et al., 2024). Their product is small whenever either factor is small, identifying submodules whose residual contribution is well approximated by near-identity surrogates of the form from Eq. (3). We select Attention modules with the lowest impact scores, aggregated robustly across calibration tokens. On the other hand, FFN selection differs between base and instruction-tuned models. For base models, we use a *replacement-aware* score that combines the effect of removing the FFN contribution with the residual error of the fitted surrogate, in the spirit of reconstruction-error importance (Frantar and Alistarh, 2023; Sun et al., 2024). For instruction-tuned models, we find that FFN residual magnitudes after SFT can be poorly calibrated across depths, making norm-based factors noisy (Harada et al., 2025); we therefore use a cosine-only score, also used in ReplaceMe (Shopkhoev et al., 2025), retaining only the cosine factor of Eq. (1).

**Fitted residual replacement.** For each selected submodule, we fit a parametric surrogate  $\tilde{F}_\ell(\cdot; \theta_\ell)$ , defined in detail in the next paragraph, by minimizing the residual error on calibration pairs:

$$\theta_\ell^* = \arg \min_{\theta_\ell} \sum_{i=1}^N \|\tilde{F}_\ell(x_i; \theta_\ell) - y_i\|_2^2, \quad (2)$$

with  $\theta_\ell^*$  recovered analytically from calibration statistics, without full-model fine-tuning, in the spirit of activation-driven post-training compression (Frantar and Alistarh, 2023; Sun et al., 2024; Ashkboos et al., 2024).

**A common submodule surrogate.** Both Attention and FFN submodules contribute to the residual stream via an additive map  $\mathbb{R}^d \rightarrow \mathbb{R}^d$  (Vaswani

et al., 2017); since each submodule  $F_\ell$  communicates with the rest of the network only through this output, we approximate it through its input-output signature rather than reproducing its internal computation. For both kinds of submodels, we use the same surrogate structure:

$$\tilde{F}_\ell(x; \theta_\ell) = \underbrace{g_\ell \odot x + b_\ell}_{\text{affine correction}} + \underbrace{(x - \mu_\ell) U_\ell}_{\text{structured interaction}}, \quad (3)$$

where  $\theta_\ell = \{g_\ell, b_\ell, \mu_\ell, U_\ell\}$  collects all layer specific parameters,  $\odot$  denotes the element-wise (Hadamard) product, and  $U_\ell \in \mathbb{R}^{d \times d}$  is a low-rank operator constrained by  $\text{rank}(U_\ell) \leq r$ , factored as:

$$U_\ell = V_\ell^\top W_\ell, \quad V_\ell, W_\ell \in \mathbb{R}^{r \times d}. \quad (4)$$

Each component plays a distinct role. The element-wise gate  $g_\ell$  restores the per-feature scale of the removed contribution, accounting for the fact that different hidden dimensions are written into the residual stream with different magnitudes. The bias  $b_\ell$  and the centering term  $\mu_\ell$  together absorb the mean shift induced by removing the original submodule output (Chen et al., 2026b):  $\mu_\ell$  re-centers the input around the calibration mean so that the low-rank operator models only zero-mean variation, while  $b_\ell$  restores the target mean at the output. Finally,  $U_\ell$  captures structured cross-feature interactions that the diagonal gate cannot represent, in a low-rank form, motivated by intrinsic dimensionality results for Transformer adaptation (Aghajanyan et al., 2021; Hu et al., 2022); the overall linear form reflects the empirical near-linearity of per-layer transitions in Transformer decoders (Razzhigaev et al., 2024). Because  $\tilde{F}_\ell$  matches the input/output signature of  $F_\ell$ , the surrounding Transformer block is left unchanged (Shopkoev et al., 2025). The two submodule types differ only in (i) the supervision target  $y_i = F_\ell(x_i)$  and (ii) whether the rank- $r$  input basis  $V_\ell$  is layer-specific or shared across layers.

**Closed-form rank- $r$  fit.** The surrogate in Eq. (3) admits a closed-form fitting procedure on calibration statistics, with no gradient-based optimization. Setting  $\mu_\ell$  to the empirical input mean and  $b_\ell$  to the empirical target mean decouples the affine and low-rank components (Frisch–Waugh–Lovell theorem): with  $(\mu_\ell, b_\ell)$  fixed, the residual problem in  $(g_\ell, U_\ell)$  is expressed entirely on centered quantities, and the two terms in Eq. (3) no longer share their constant component. The element-wise gate is then recovered per feature as the ridge-regularized univariate

slope

$$g_\ell^{(j)} = \frac{\tilde{\sigma}_{xy}^{(j)}}{\tilde{\sigma}_{xx}^{(j)} + \lambda}, \quad (5)$$

where  $\tilde{\sigma}_{xx}^{(j)}$  and  $\tilde{\sigma}_{xy}^{(j)}$  are the centered input variance and input-target covariance on coordinate  $j$ , respectively, and  $\lambda > 0$  is a small ridge term. Conditioned on  $(g_\ell, b_\ell, \mu_\ell)$ , the low-rank operator  $U_\ell = V_\ell^\top W_\ell$  is fit in two steps. The input basis  $V_\ell$  is set to the top- $r$  eigenvectors of the centered input covariance  $\tilde{\Sigma}_{xx}^{(\ell)} = \tilde{X}_\ell^\top \tilde{X}_\ell$ , which selects the  $r$ -dimensional subspace of inputs along which the calibration activations carry most of their variance; this leverages the intrinsic low-dimensionality of Transformer activations (Aghajanyan et al., 2021; Hu et al., 2022). Conditioned on  $V_\ell$ , the output factor  $W_\ell$  is then recovered by ridge-regularized least squares of the affine-corrected target onto the projection of the centered input on  $V_\ell$ . The full fit thus reduces, per submodule, to one accumulation of input covariance and cross-covariance statistics, one symmetric eigen-decomposition of size  $d \times d$ , and one rank- $r$  ridge regression.

**Attention replacement (independent bases).** For a selected Attention submodule, the target  $y_i$  is the dense Attention output after the architecture-specific output projection. We instantiate Eq. (3) with a per-layer factorization  $U_\ell^{\text{attn}} = V_\ell^\top W_\ell$ , so each removed Attention submodule owns its full parameter set  $\theta_\ell^{\text{attn}} = \{g_\ell, b_\ell, \mu_\ell, V_\ell, W_\ell\}$ . This reflects the fact that Attention contributions across depths perform heterogeneous roles (He et al., 2024; Zhong et al., 2025).

**FeedForward replacement (shared input basis).** For a selected FFN submodule, the target  $y_i$  is the dense residual output after projection back to the hidden size. A naïve instantiation of Eq. (3) would assign an independent basis  $V_\ell$  to each removed submodule. Instead, SUBFIT ties the input basis across  $\ell \in \mathcal{S}_{\text{fn}}$ , setting  $U_\ell^{\text{fn}} = V^\top W_\ell$  with a single  $V \in \mathbb{R}^{r \times d}$  shared across selected layers; only  $\theta_\ell^{\text{fn}} = \{g_\ell, b_\ell, \mu_\ell, W_\ell\}$  remains layer-specific. This realizes a cross-layer parameter-sharing structure (Mikaelyan et al., 2025), i.e., a common  $r$ -dimensional input subspace across the removed submodules, with per-layer output coefficients  $W_\ell$  specializing the map. We estimate the shared-basis surrogate from joint calibration statistics:

$$\min_{V, \{\theta_\ell\}_{\ell \in \mathcal{S}_{\text{fn}}}} \sum_{\ell \in \mathcal{S}_{\text{fn}}} \sum_{i=1}^N \|\tilde{F}_\ell^{\text{fn}}(x_i^{(\ell)}) - y_i^{(\ell)}\|_2^2, \quad (6)$$

In practice,  $V$  is set to the top- $r$  eigenvectors of the sum of centered input covariances across all selected FFN layers; each  $W_\ell$  is then recovered by an independent ridge least-squares. The shared basis is thus estimated once from joint statistics, while output coefficients remain layer-specific.

A second source of parameter savings comes from the surrogate operating directly on the residual stream of dimension  $d$ , bypassing the larger inner dimension  $d_{ff} \gg d$  of the FFN block. Since a SwiGLU (Shazeer, 2020) FFN comprises three  $d \times d_{ff}$  projections (gate, up, down) per selected layer, the bypass stores  $W_\ell \in \mathbb{R}^{r \times d}$  together with the three  $d$ -dimensional vectors  $g_\ell, b_\ell, \mu_\ell$ , totaling  $rd + 3d$  parameters, plus the shared  $V \in \mathbb{R}^{r \times d}$  amortized across all  $|\mathcal{S}_{fn}|$  selected layers. Compared to the  $3dd_{ff}$  parameters of the original block, the layer-specific parameter count is roughly  $10\times$  smaller at  $r = d$  for typical decoder LLMs with  $d_{ff} \approx 3.5d$ .

**Deployment form.** After fitting, each selected submodule is replaced by its corresponding residual bypass, which approximates only the net residual contribution of the original submodule rather than its internal computation. The original model weights outside the selected submodules are left unchanged. For FFNs, the shared basis is stored once and reused across selected layers, while the layer-specific affine terms and output factors are stored per layer. This gives SUBFIT a compact deployed form relative to the removed submodules, while preserving a separate residual approximation for each removed component (see Table A9).

## 4 Experiments

In this section, we describe the experimental setup and the numerical results of SUBFIT relative to the selected baselines. We organize our evaluation around three research questions: **(RQ1)**: How does submodule-level replacement, like SUBFIT, compare to layer-level replacement on perplexity and downstream accuracy? **(RQ2)**: How does SUBFIT scale with sparsity? and **(RQ3)**: How does SUBFIT translate into inference-time efficiency?

**Experimental Setup.** We outline the key design choices and evaluation protocol below; full details on models, sparsity grid, datasets, metrics, and calibration are provided in Section C. Note that GSM8K is reported separately in Section A.4, due to its known sensitivity to prompting (Sclar et al., 2024) and instability under compression of genera-

Table 1: Perplexity comparison at representative sparsity levels. Lower PPL is better; PPL Deg. is the geometric mean of sparse/dense PPL ratios.

Sparsity	Method	Lambda ↓	C4 ↓	WikiText2 ↓	PPL Deg. ↓
<b>Llama-3.2-3B</b>					
Dense		20.15	11.07	7.82	1.00×
12.5%	Streamline (FFN)	31.65	19.48	18.73	1.88×
	Streamline (Layer)	27.92	18.59	16.66	1.71×
	ReplaceMe (LS)	28.35	18.41	13.33	1.59×
	ReplaceMe (Cosine)	27.84	18.34	13.30	1.57×
	<b>SUBFIT</b>	<b>27.25</b>	<b>15.96</b>	<b>10.81</b>	<b>1.39×</b>
25%	Streamline (FFN)	51.22	36.68	42.96	3.59×
	Streamline (Layer)	47.93	33.62	38.35	3.28×
	ReplaceMe (LS)	52.15	36.35	44.07	3.63×
	ReplaceMe (Cosine)	50.22	31.34	23.47	2.77×
	<b>SUBFIT</b>	<b>39.17</b>	<b>23.42</b>	<b>17.86</b>	<b>2.11×</b>
<b>Qwen3-4B</b>					
Dense		33.80	19.89	13.67	1.00×
12.5%	Streamline (FFN)	46.78	28.83	25.28	1.55×
	ReplaceMe (LS)	48.74	30.86	24.55	1.59×
	ReplaceMe (Cosine)	45.40	28.56	20.70	1.43×
	<b>SUBFIT</b>	<b>39.40</b>	<b>23.87</b>	<b>19.86</b>	<b>1.27×</b>
25%	Streamline (FFN)	448.64	329.13	1451.81	28.57×
	Streamline (Layer)	314.53	282.55	1264.41	23.04×
	ReplaceMe (LS)	151.88	120.50	201.71	7.38×
	ReplaceMe (Cosine)	132.37	93.01	115.85	5.37×
	<b>SUBFIT</b>	<b>69.26</b>	<b>43.52</b>	<b>50.08</b>	<b>2.54×</b>
<b>Llama-3.1-8B</b>					
Dense		17.78	9.36	6.24	1.00×
12.5%	Streamline (FFN)	22.10	14.07	10.00	1.44×
	Streamline (Layer)	<b>21.65</b>	13.75	9.76	1.41×
	ReplaceMe (LS)	22.35	14.19	9.52	1.43×
	ReplaceMe (Cosine)	22.14	14.16	9.46	1.42×
	<b>SUBFIT</b>	<b>24.24</b>	<b>13.57</b>	<b>8.63</b>	<b>1.40×</b>
25%	Streamline (FFN)	35.90	25.60	20.84	2.64×
	Streamline (Layer)	33.88	24.84	19.30	2.50×
	ReplaceMe (LS)	43.28	29.84	32.25	3.42×
	ReplaceMe (Cosine)	54.63	34.60	31.29	3.85×
	<b>SUBFIT</b>	<b>33.09</b>	<b>19.30</b>	<b>14.23</b>	<b>2.06×</b>
<b>Qwen3-8B</b>					
Dense		25.70	15.25	9.72	1.00×
12.5%	Streamline (FFN)	37.52	23.84	20.65	1.69×
	Streamline (Layer)	36.30	22.78	<b>15.88</b>	1.51×
	ReplaceMe (LS)	38.69	25.96	24.99	1.87×
	ReplaceMe (Cosine)	37.05	24.83	21.37	1.73×
	<b>SUBFIT</b>	<b>34.32</b>	<b>20.13</b>	17.03	<b>1.46×</b>
25%	Streamline (FFN)	356.48	348.07	1332.92	35.14×
	Streamline (Layer)	229.51	204.43	855.48	21.92×
	ReplaceMe (LS)	112.81	89.45	177.44	7.77×
	ReplaceMe (Cosine)	102.44	77.96	150.20	6.80×
	<b>SUBFIT</b>	<b>63.22</b>	<b>40.06</b>	<b>48.52</b>	<b>3.18×</b>
<b>DeepSeek-7B</b>					
Dense		14.36	9.75	6.85	1.00×
12.5%	Streamline (FFN)	20.37	15.16	12.23	1.58×
	Streamline (Layer)	19.33	14.47	10.77	1.46×
	ReplaceMe (LS)	18.75	14.26	11.09	1.46×
	ReplaceMe (Cosine)	<b>18.21</b>	<b>14.12</b>	10.65	<b>1.42×</b>
	<b>SUBFIT</b>	23.17	14.47	<b>9.95</b>	1.52×
25%	Streamline (FFN)	45.88	38.77	39.20	4.17×
	Streamline (Layer)	35.37	29.38	26.06	3.05×
	ReplaceMe (LS)	34.35	29.64	28.42	3.11×
	ReplaceMe (Cosine)	41.79	35.28	40.95	3.98×
	<b>SUBFIT</b>	<b>31.35</b>	<b>21.44</b>	<b>18.94</b>	<b>2.37×</b>

tive reasoning (Shrestha et al., 2026).

We compare against four post-training, calibration-only block-replacement baselines that share the two design constraints relaxed by SUBFIT: **Streamline (FFN)** and **Streamline**

Table 2: Downstream performance (%) at sparsity 25%. Acc. Ret. is the ratio sparse/dense aggregate accuracy.

Model	Sparsity	Commonsense					QA		Knowledge	Reasoning		Math	Science	Average	
		HS	PIQA	Wino	OBQA	SIQA	BoolQ	TQA	MMLU	ARC-C	ARC-E	MathQA	SciQ	Avg	Acc. Ret.
<b>Llama-3.2-3B-Instruct</b>	Dense	64.53	75.63	67.88	42.00	46.11	75.63	33.54	61.84	45.31	68.10	26.03	87.90	57.87	100.00%
Streamline (FFN)		50.25	64.58	67.09	30.80	41.30	76.42	28.89	34.45	33.62	47.39	21.78	68.30	47.07	81.33%
Streamline (Layer)		50.93	65.40	66.38	30.00	41.56	79.24	29.62	55.05	34.90	48.23	21.57	71.40	49.52	85.57%
ReplaceMe (LS)	25%	48.84	63.71	65.51	32.60	40.48	79.20	27.66	61.31	30.97	49.16	<b>22.48</b>	75.00	49.74	85.95%
ReplaceMe (Cosine)		50.45	<b>65.51</b>	<b>67.25</b>	32.20	40.79	<b>79.30</b>	30.35	<b>61.35</b>	31.91	47.60	22.28	75.80	50.40	87.08%
SUBFIT		<b>51.42</b>	<b>65.51</b>	65.35	<b>34.20</b>	<b>41.97</b>	77.13	<b>31.33</b>	60.69	<b>34.98</b>	<b>51.60</b>	22.18	<b>80.00</b>	<b>51.36</b>	<b>88.75%</b>
<b>Qwen3-4B-Instruct</b>	Dense	43.42	69.70	56.75	40.80	46.32	84.83	39.17	72.18	43.17	55.43	33.30	67.50	54.38	100.00%
Streamline (FFN)		22.93	49.95	42.23	33.80	34.54	62.26	24.60	<b>71.74</b>	26.28	27.61	25.26	22.80	37.00	68.04%
Streamline (Layer)		22.63	54.95	<b>57.62</b>	31.20	39.00	62.17	32.19	59.23	<b>31.57</b>	40.28	25.49	37.00	41.11	75.60%
ReplaceMe (LS)	25%	<b>37.05</b>	<b>66.43</b>	52.88	<b>37.20</b>	38.59	50.61	<b>34.88</b>	31.05	31.40	<b>41.71</b>	<b>25.63</b>	51.60	41.59	76.47%
ReplaceMe (Cosine)		36.72	66.32	54.30	35.20	38.69	52.11	33.66	31.56	29.78	40.36	24.25	49.80	41.06	75.51%
SUBFIT		28.88	55.01	54.93	33.20	<b>40.02</b>	<b>63.64</b>	34.64	64.23	29.01	36.03	24.69	<b>60.90</b>	<b>43.76</b>	<b>80.48%</b>
<b>Qwen2.5-7B-Instruct</b>	Dense	65.48	73.50	61.01	44.00	45.75	85.81	47.49	73.51	43.34	50.84	34.17	55.40	56.69	100.00%
Streamline (FFN)		51.87	71.93	52.88	39.00	40.84	60.31	28.76	27.67	33.96	<b>44.78</b>	27.71	<b>56.30</b>	44.67	78.79%
Streamline (Layer)		53.10	<b>72.36</b>	56.51	40.80	41.45	59.91	27.30	28.11	34.98	44.07	27.47	54.80	45.07	79.50%
ReplaceMe (LS)	25%	52.47	70.73	56.35	39.80	41.66	65.05	28.52	31.80	<b>35.67</b>	42.89	<b>29.58</b>	50.50	45.42	80.11%
ReplaceMe (Cosine)		<b>53.17</b>	71.49	56.51	<b>41.40</b>	<b>42.48</b>	65.20	29.25	32.86	34.56	42.34	28.44	51.60	<b>45.77</b>	<b>80.74%</b>
SUBFIT		48.19	69.26	<b>57.85</b>	40.20	41.91	<b>68.10</b>	<b>33.66</b>	<b>35.59</b>	34.13	41.79	27.84	49.40	45.66	80.54%
<b>DeepSeek-7B-chat</b>	Dense	70.56	77.64	74.90	44.80	50.46	83.98	37.21	50.90	41.55	62.63	27.54	78.40	58.38	100.00%
Streamline (FFN)		39.83	61.48	65.35	32.80	38.38	63.46	<b>30.84</b>	39.77	<b>34.98</b>	39.48	20.94	38.50	42.15	72.20%
Streamline (Layer)		50.02	66.32	<b>70.95</b>	<b>35.60</b>	44.37	64.01	27.54	48.68	31.14	44.07	21.88	58.50	46.92	80.37%
ReplaceMe (LS)	25%	47.15	63.77	70.88	35.20	43.50	75.84	29.25	48.94	32.51	42.72	22.81	48.20	46.73	80.05%
ReplaceMe (Cosine)		<b>50.70</b>	<b>71.60</b>	55.41	35.40	41.56	59.48	27.05	25.46	27.90	<b>47.98</b>	24.22	<b>73.50</b>	45.02	77.12%
SUBFIT		48.64	65.02	70.72	34.00	<b>46.37</b>	<b>83.09</b>	29.74	<b>49.96</b>	33.11	46.13	<b>24.62</b>	58.40	<b>49.15</b>	<b>84.19%</b>
<b>Llama-3.1-8B-Instruct</b>	Dense	72.52	79.49	77.82	49.00	50.20	83.88	40.39	68.79	53.58	75.76	26.80	91.70	64.16	100.00%
Streamline (FFN)		58.31	68.82	74.35	34.80	43.71	<b>84.59</b>	33.05	67.54	38.48	54.71	22.35	77.40	54.84	85.47%
Streamline (Layer)		59.90	<b>70.46</b>	<b>75.22</b>	34.00	44.01	84.56	33.90	67.77	<b>40.19</b>	56.82	22.18	80.20	55.77	86.92%
ReplaceMe (LS)	25%	57.27	67.90	72.61	35.60	44.01	84.56	34.39	<b>68.00</b>	38.74	54.67	21.24	75.50	54.54	85.01%
ReplaceMe (Cosine)		<b>60.22</b>	70.08	72.85	37.20	45.34	84.37	35.99	67.95	40.02	57.41	21.61	76.00	55.75	86.89%
SUBFIT		59.33	69.48	<b>75.22</b>	<b>39.20</b>	<b>45.96</b>	84.43	<b>36.23</b>	67.27	39.93	<b>59.85</b>	<b>23.22</b>	<b>84.10</b>	<b>57.02</b>	<b>88.87%</b>

(Layer) (Chen et al., 2025b), which replace a contiguous block of selected layers with a trained feed-forward network or a full Transformer layer, respectively; **ReplaceMe (LS)** and **ReplaceMe (Cosine)** (Shophkoev et al., 2025), which fit a single linear transformation for the contiguous removed blocks, folded into existing weights at deployment<sup>1</sup>. All methods use the same calibration data (SlimPajama (Shen et al., 2023) for base models and SlimOrca (Mukherjee et al., 2023) for instruction-tuned models, 8k samples at sequence length 1024. For SUBFIT, we use rank 256 for Attention bypasses and rank 4096 for the shared FFN basis (see Section 5).

**RQ1: Perplexity and accuracy at the submodule-level.** We analyze how SUBFIT is positioned on the perplexity–accuracy trade-off relative to the four replacement-based baselines. Base-model perplexity (Table 1) and instruction-tuned downstream accuracy (Table 2) report the two axes at representative sparsity levels; the remaining sparsities are deferred to Section A.1 and Section A.2.

Considering perplexity, SUBFIT attains the lowest PPL degradation in 9 of 10 model–sparsity settings reported in Table 1, and is consistently strongest at 25% sparsity. The separation is most pronounced on the Qwen family, where contiguous

replacement baselines degrade sharply: at 25% sparsity, the strongest ReplaceMe baseline reaches  $5.37\times$  on Qwen3-4B and  $6.80\times$  on Qwen3-8B, while SUBFIT reduces these to  $2.54\times$  and  $3.18\times$  respectively. On the Llama and DeepSeek families, the ordering is the same, with SUBFIT consistently best at 25% sparsity.

On the accuracy side, SUBFIT obtains the best aggregate downstream accuracy on 4 of 5 models at 25% sparsity (Table 2), retaining 84.6% of dense performance on average. The single exception is Qwen2.5-7B-Instruct, where ReplaceMe Cosine is marginally higher in aggregate (+0.11%); even there, SUBFIT improves several individual tasks, including Winogrande (Sakaguchi et al., 2021), BoolQ (Clark et al., 2019), TruthfulQA (Lin et al., 2022), and MMLU (Hendrycks et al., 2021). At 25% sparsity, it provides the strongest aggregate trade-off between base-model PPL degradation and instruction-tuned accuracy retention (Figure 1).

**RQ2: Scaling with compression.** Table 3 aggregates accuracy retention over instruction-tuned models and PPL degradation over base models across all five sparsity levels. At the aggregate level, SUBFIT attains the strongest score on both axes at every evaluated sparsity level, and the margin over the strongest competing baseline widens monotonically with compression: the PPL gap grows

<sup>1</sup>See Section C for details on the choice of the baselines.

from  $0.11\times$  at 12.5% to  $1.92\times$  at 25% and  $5.69\times$  at 37.5%, while accuracy retention separates by +0.2, +3.0, and +3.0 points at the same sparsities. SUBFIT is also the only method to retain above 80% accuracy at 25% and above 73% at 37.5%. Stability follows the same pattern: PPL-factor standard deviation stays bounded for SUBFIT ( $\pm 0.08 \rightarrow \pm 1.37$ ), whereas baselines grow by one to two orders of magnitude (e.g. ReplaceMe Cosine reaches  $\pm 130.68$  at 37.5%). These results suggest that submodule-level non-contiguous selection can extend the usable compression range, rather than only shifting the trade-off curve at a fixed operating point.

Table 3: Aggregate compression trade-off across sparsity levels (avg $\pm$ std). Accuracy retention is averaged over instruction-tuned models; PPL factor is averaged over base models, with each model-level factor computed from Lambada, C4, and WikiText-2.

Accuracy retention (%) $\uparrow$					
Method	12.5%	20%	25%	30%	37.5%
Streamline (FFN)	91.7 $\pm$ 3.1	86.2 $\pm$ 4.3	77.2 $\pm$ 6.3	72.3 $\pm$ 7.9	64.8 $\pm$ 5.8
Streamline (Layer)	93.2 $\pm$ 2.3	85.4 $\pm$ 3.5	81.6 $\pm$ 4.1	74.9 $\pm$ 7.0	68.7 $\pm$ 6.4
ReplaceMe (LS)	92.7 $\pm$ 1.8	85.8 $\pm$ 4.2	81.5 $\pm$ 3.5	77.7 $\pm$ 4.7	70.8 $\pm$ 5.6
ReplaceMe (Cosine)	93.2 $\pm$ 2.4	86.8 $\pm$ 4.0	81.5 $\pm$ 4.8	79.1 $\pm$ 4.0	70.9 $\pm$ 5.6
SUBFIT	<b>93.4<math>\pm</math>2.7</b>	<b>88.1<math>\pm</math>3.4</b>	<b>84.6<math>\pm</math>3.7</b>	<b>80.8<math>\pm</math>3.8</b>	<b>73.9<math>\pm</math>2.9</b>
PPL factor ( $\times$ dense) $\downarrow$					
Method	12.5%	20%	25%	30%	37.5%
Streamline (FFN)	1.62 $\pm$ 1.5	2.43 $\pm$ 7.0	8.31 $\pm$ 14.07	7.06 $\pm$ 3.09	16.01 $\pm$ 14.17
Streamline (Layer)	1.52 $\pm$ 1.1	2.50 $\pm$ 6.1	6.61 $\pm$ 9.58	6.61 $\pm$ 4.96	12.44 $\pm$ 13.21
ReplaceMe (LS)	1.58 $\pm$ 1.6	2.82 $\pm$ 1.17	4.67 $\pm$ 2.06	8.09 $\pm$ 5.86	11.45 $\pm$ 10.01
ReplaceMe (Cosine)	1.51 $\pm$ 1.2	2.46 $\pm$ 7.5	4.34 $\pm$ 1.40	7.38 $\pm$ 7.99	22.28 $\pm$ 130.68
SUBFIT	<b>1.40<math>\pm</math>0.8</b>	<b>1.81<math>\pm</math>2.2</b>	<b>2.42<math>\pm</math>4.0</b>	<b>3.22<math>\pm</math>5.1</b>	<b>5.76<math>\pm</math>1.37</b>

**RQ3: Inference efficiency.** Table 4 reports inference diagnostics comparing dense and SUBFIT-compressed variants on a single NVIDIA A100 80GB GPU. At 25% sparsity, time-to-first-token (TTFT) speedup over the dense model ranges from  $1.18\times$  (Llama-3.2-3B) to  $1.40\times$  (DeepSeek-7B), with decode speedup between  $1.12\times$  and  $1.17\times$ . As expected, KV-cache usage scales proportionally with sparsity, due to the complete removal of Attention submodules. These gains are consistent with the reduction in active Attention and FFN submodules, without hardware-specific optimization.

## 5 Ablation Studies

To analyze the contribution of each design choice, we conduct four ablation studies at 25% sparsity on Llama-3B and Qwen3-4B, reporting perplexity on Lambada, C4, and WikiText-2 for base models and a reduced five-task subset for instruction-tuned

Table 4: Inference speedup and KV-cache reduction. TTFT uses one generated token; decode uses 128 tokens; KV-cache is measured with a 512-token prompt.

Model	Sparsity	TTFT $\uparrow$	Decode $\uparrow$	KV-cache (MB, % saved)
Llama-3.2-3B	12.5%	1.13 $\times$	1.06 $\times$	56 $\rightarrow$ 48 (14.3%)
	25.0%	1.18 $\times$	1.12 $\times$	56 $\rightarrow$ 42 (25.0%)
	37.5%	1.22 $\times$	1.18 $\times$	56 $\rightarrow$ 36 (35.7%)
Qwen3-4B	12.5%	1.10 $\times$	1.06 $\times$	72 $\rightarrow$ 64 (11.1%)
	25.0%	1.18 $\times$	1.17 $\times$	72 $\rightarrow$ 54 (25.0%)
	37.5%	1.30 $\times$	1.27 $\times$	72 $\rightarrow$ 44 (38.9%)
Llama-3.1-8B	12.5%	1.17 $\times$	1.06 $\times$	64 $\rightarrow$ 56 (12.5%)
	25.0%	1.26 $\times$	1.13 $\times$	64 $\rightarrow$ 48 (25.0%)
	37.5%	1.33 $\times$	1.20 $\times$	64 $\rightarrow$ 40 (37.5%)
Qwen3-8B	12.5%	1.15 $\times$	1.07 $\times$	72 $\rightarrow$ 64 (11.1%)
	25.0%	1.24 $\times$	1.17 $\times$	72 $\rightarrow$ 54 (25.0%)
	37.5%	1.37 $\times$	1.29 $\times$	72 $\rightarrow$ 44 (38.9%)
DeepSeek-7B	12.5%	1.31 $\times$	1.05 $\times$	240 $\rightarrow$ 208 (13.3%)
	25.0%	1.40 $\times$	1.12 $\times$	240 $\rightarrow$ 176 (26.7%)
	37.5%	1.49 $\times$	1.16 $\times$	240 $\rightarrow$ 152 (36.7%)

models (with *Inst. Avg.* interpreted as a relative indicator within this section).

**Residual compensation.** Table 5 isolates the role of residual compensation. *Pruning only* removes the selected submodules without any replacement, leading to severe degradation, which confirms that naïve deletion is not viable at this sparsity. Compensating Attention alone (*w/ Attn.*) improves over pruning-only but still suffers high degradation, whereas compensating FFNs alone (*w/ FeedForward*) recovers most of the degradation. This suggests that approximating removed FFN residuals is the dominant factor for stability in this setting. The full SUBFIT configuration (*w/ Attn. + FeedForward*) yields the best downstream accuracy on both models, with Qwen3-4B base PPL slightly favoring FeedForward-only compensation. This asymmetry motivates SUBFIT’s design: per-layer parameters for Attention, and a shared input basis across FFNs.

Table 5: Residual compensation component ablation at 25% sparsity without cross-task aggregation. Base rows report raw task-wise PPL; instruction-tuned rows report raw downstream average accuracy. Large PPL values are shown in scientific notation.

Model	Setup	Base PPL $\downarrow$			Inst. Avg. $\uparrow$
		LAMB.	C4	WT2	
Llama-3B	Pruning only	$1.30 \times 10^4$	$1.01 \times 10^4$	$1.12 \times 10^4$	60.8
	w/ Attn. comp.	$5.32 \times 10^3$	$9.52 \times 10^3$	$1.11 \times 10^4$	62.2
	w/ FeedForward comp.	<b>37.42</b>	22.94	16.98	67.7
	w/ Attn.+FeedForward (Ours)	<b>37.82</b>	<b>22.26</b>	<b>16.57</b>	<b>69.5</b>
Qwen3-4B	Pruning only	212	92.33	79.27	50.9
	w/ Attn. comp.	82.92	53.58	67.73	48.0
	w/ FeedForward comp.	74.60	48.13	<b>39.71</b>	55.6
	w/ Attn.+FeedForward (Ours)	<b>69.36</b>	<b>43.49</b>	50.10	<b>56.9</b>

**Shared versus per-layer FeedForward basis.** Table 6 compares the shared FFN basis used by SUB-

FIT against a per-layer basis variant, applied to the same selected FFN layers. Across all base-model PPL metrics, differences are at most 0.01 in raw perplexity, and instruction-tuned averages differ by at most 0.2 accuracy points. At the same time, the per-layer variant stores an independent  $V_\ell \in \mathbb{R}^{r \times d}$  for each removed layer, while the shared variant stores a single  $V$  reused across all selected FFNs, reducing the basis cost by a factor of  $|\mathcal{S}_{\text{fn}}|$ . The shared design, therefore, matches the per-layer variant while using much fewer deployed parameters.

Table 6: Shared versus per-layer FeedForward basis at 25% sparsity under fixed selected layers.

Model	Basis	Base PPL ↓			Inst. Avg. ↑
		LAMB.	C4	WT2	
Llama-3B	Per-layer	<b>33.55</b>	<b>19.95</b>	14.01	<b>72.7</b>
	Shared (Ours)	<b>33.55</b>	19.96	<b>14.00</b>	<b>72.5</b>
Qwen3-4B	Per-layer	50.01	<b>28.95</b>	<b>19.11</b>	<b>66.7</b>
	Shared (Ours)	<b>50.00</b>	28.97	19.12	<b>66.6</b>

**Rank sensitivity.** We sweep Attention and FFN bypass ranks independently, holding the selected layers fixed to isolate rank effects from layer-selection effects. As shown in Figure 3, the two submodule types exhibit qualitatively different behavior: FFN quality improves steadily and plateaus around rank 4096, suggesting that a higher-dimensional shared input subspace is beneficial to capture the residual contribution of removed FFNs, whereas Attention saturates already at rank 256, suggesting a low-rank operator suffices. SUBFIT therefore uses rank 256 for Attention bypasses and rank 4096 for the shared FFN basis, matching each submodule to the smallest rank past which gains plateau.

### Replacement-aware vs. masked scoring.

We compare deletion-only scoring with post-replacement scoring to test whether masked degradation is a reliable proxy for replacement quality. Table 7 shows that the two criteria often select different scores: the criterion that minimizes masked degradation is not always the one that yields the best post-replacement outcome. This mismatch appears across both tested model families and submodule types, suggesting that replacement quality depends not only on the local effect of masking a submodule, but also on how well its residual contribution can be approximated by the surrogate.

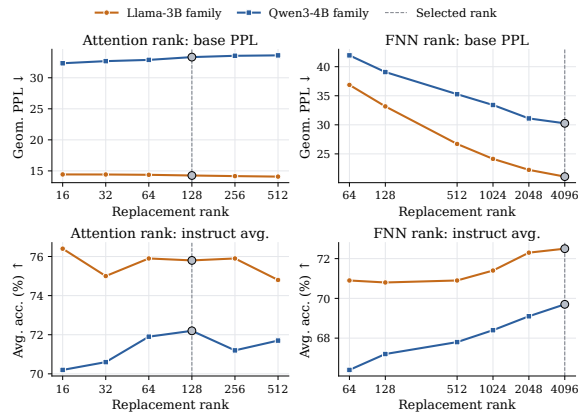


Figure 3: Fixed-selection rank sensitivity at 25% sparsity. FFN quality improves steadily up to rank 4096, while Attention saturates already at rank 256, confirming that the two submodule types require different ranks.

Table 7: Masked degradation and post replacement quality disagree in 5 of 8 cases (marked ×), indicating that masked degradation is not a reliable proxy for replacement quality.

Model	Block	Preferred masked	Preferred replaced	Match
<i>Base models: WikiText-2 PPL ↓</i>				
Llama-3B	Attn.	Impact (10.07)	Impact (9.50)	✓
Llama-3B	FeedForward	Cosine (45.28)	Impact (14.01)	×
Qwen3-4B	Attn.	Impact (36.66)	Cosine (24.11)	×
Qwen3-4B	FeedForward	Impact (23.56)	Impact (19.12)	✓
<i>Instruction-tuned: Avg. Acc. ↑</i>				
Llama-3B-Inst.	Attn.	Cosine (74.8)	Cosine (76.2)	✓
Llama-3B-Inst.	FeedForward	Tie (63.7)	Cosine (73.0)	×
Qwen3-4B-Inst.	Attn.	Cosine (69.4)	Impact (71.1)	×
Qwen3-4B-Inst.	FeedForward	Tie (58.4)	Cosine (68.6)	×

## 6 Conclusion

This work asked whether the granularity at which replacement-based compression methods operate is itself a design choice that can be improved. Our results suggest that this granularity can be improved: selecting Attention and FFN submodules independently across depths, and replacing each with a fitted residual bypass, recovers more of the dense model’s behavior than contiguous full-layer replacement under the same parameter budget.

The asymmetric nature of the recovery, where FFN compensation accounts for most of the recovered quality and Attention compensation refines the residual, also justifies the asymmetric design of SUBFIT: per-layer parameters for Attention, a shared input basis for FFNs. The closed-form fit on calibration statistics makes the method cheap to deploy and easy to combine with existing inference stacks, with no sparse kernels or custom hardware required. The result that submodule-level recov-

ery provides a stronger aggregate trade-off than layer-level recovery in our evaluated settings suggests that granularity is an underexplored axis in post-training compression, one that may generalize to other removal units such as attention heads or individual neurons.

## Limitations

SUBFIT introduces explicit bypass parameters for selected Attention and FFN submodules, adding approximately 10% of removed parameters and 15% of removed MACs at 25% sparsity (Table A9 and Table A10 in the Appendix). This overhead is stable across sparsity levels. In contrast, ReplaceMe (Shopkhoev et al., 2025) variants add no deployed parameters as their transformations are folded into existing weights. The offline compression pipeline requires approximately 2,000–2,600 seconds on average, comparable to ReplaceMe Cosine but slower than Streamline (Chen et al., 2025b), due to sequential selection and closed-form fitting. This cost is incurred once at compression time and does not affect deployed inference latency.

## Ethical Considerations

This work focuses on post-training compression for large language models. All models, datasets, and benchmarks used in our experiments are publicly available, and we credit the original authors throughout the manuscript. Our method does not introduce new training data or collect user data; it operates on pretrained models using calibration samples to fit lightweight replacement modules. As with other model-compression techniques, SUBFIT can make LLM deployment cheaper and more accessible. This may broaden beneficial uses of language models, but it may also lower the cost of deploying models in harmful or unintended applications. Our work addresses the technical problem of deployable compression and does not target any specific downstream application. Compression may also affect model behavior unevenly across tasks, domains, or demographic groups. To reduce the risk of hiding such effects, we report performance across multiple benchmarks, model families, and sparsity levels, and we separately discuss unstable settings such as GSM8K. However, our evaluation does not constitute a complete fairness or safety audit of compressed models. Further task-specific evaluation is needed before deploying compressed models in high-stakes settings.

## References

Armen Aghajanyan, Sonal Gupta, and Luke Zettlemoyer. 2021. *Intrinsic Dimensionality Explains the Effectiveness of Language Model Fine-Tuning*. In *Proceedings of the 59th Annual Meeting of the Association for Computational Linguistics and the 11th*

*International Joint Conference on Natural Language Processing (Volume 1: Long Papers)*, pages 7319–7328, Online. Association for Computational Linguistics.

Aida Amini, Saadia Gabriel, Shanchuan Lin, Rik Koncel-Kedziorski, Yejin Choi, and Hannaneh Hajishirzi. 2019. *MathQA: Towards Interpretable Math Word Problem Solving with Operation-Based Formalisms*. In *Proceedings of the 2019 Conference of the North American Chapter of the Association for Computational Linguistics: Human Language Technologies*.

Yongqi An, Xu Zhao, Tao Yu, Ming Tang, and Jinqiao Wang. 2024. *Fluctuation-based adaptive structured pruning for large language models*. In *Proceedings of the AAAI Conference on Artificial Intelligence*, volume 38, pages 10865–10873.

Saleh Ashkboos, Maximilian Croci, Marcelo Gennari do Nascimento, Torsten Hoefer, and James Hensman. 2024. *SliceGPT: Compress Large Language Models by Deleting Rows and Columns*. In *International Conference on Learning Representations*, volume 2024, pages 11682–11701.

Xiao Bi, Deli Chen, Guanting Chen, Shanhuang Chen, Damai Dai, Chengqi Deng, Honghui Ding, Kai Dong, Qishi Du, Zhe Fu, and 1 others. 2024. *DeepSeek LLM: Scaling Open-Source Language Models with Longtermism*. *arXiv preprint arXiv:2401.02954*.

Yonatan Bisk, Rowan Zellers, Ronan Le Bras, Jianfeng Gao, and Yejin Choi. 2020. *PIQA: Reasoning about Physical Commonsense in Natural Language*. In *Proceedings of the AAAI Conference on Artificial Intelligence*.

Mengzhao Chen, Wenqi Shao, Peng Xu, Jiahao Wang, Peng Gao, Kaipeng Zhang, and Ping Luo. 2025a. *EfficientQAT: Efficient Quantization-Aware Training for Large Language Models*. In *Proceedings of the 63rd Annual Meeting of the Association for Computational Linguistics (Volume 1: Long Papers)*, pages 10081–10100.

Xiaodong Chen, Yuxuan Hu, Jing Zhang, Yanling Wang, Cuiqing Li, and Hong Chen. 2025b. *Streamlining Redundant Layers to Compress Large Language Models*. In *International Conference on Learning Representations*.

Xinrui Chen, Haoli Bai, Tao Yuan, Ruikang Liu, Kang Zhao, Xianzhi Yu, Lu Hou, Tian Guan, Yonghong He, and Chun Yuan. 2026a. *A Simple Linear Patch Revives Layer-Pruned Large Language Models*. In *Advances in Neural Information Processing Systems*.

Xinrui Chen, Hongxing Zhang, Fanyi Zeng, Yongxian Wei, Yizhi Wang, Xitong Ling, Guanghao Li, and Chun Yuan. 2026b. *Prune&Comp: Free Lunch for Layer-Pruned LLMs via Iterative Pruning with Magnitude Compensation*. *Proceedings of the AAAI Conference on Artificial Intelligence*, 40(24):20316–20324.

- Christopher Clark, Kenton Lee, Ming-Wei Chang, Tom Kwiatkowski, Michael Collins, and Kristina Toutanova. 2019. BoolQ: Exploring the Surprising Difficulty of Natural Yes/No Questions. In *Proceedings of the 2019 Conference of the North American Chapter of the Association for Computational Linguistics: Human Language Technologies*.
- Peter Clark, Isaac Cowhey, Oren Etzioni, Tushar Khot, Ashish Sabharwal, Carissa Schoenick, and Oyvind Tafjord. 2018. Think You Have Solved Question Answering? Try ARC, the AI2 Reasoning Challenge. *arXiv preprint arXiv:1803.05457*.
- Karl Cobbe, Vineet Kosaraju, Mohammad Bavarian, Mark Chen, Heewoo Jun, Lukasz Kaiser, Matthias Plappert, Jerry Tworek, Jacob Hilton, Reiichiro Nakano, Christopher Hesse, and John Schulman. 2021. Training Verifiers to Solve Math Word Problems. *arXiv preprint arXiv:2110.14168*.
- Elia Cunegatti, Leonardo Lucio Custode, and Giovanni Iacca. 2025. [Zeroth-Order Adaptive Neuron Alignment Based Pruning without Re-Training](#). *Transactions on Machine Learning Research*.
- Elias Frantar and Dan Alistarh. 2023. SparseGPT: Massive Language Models Can Be Accurately Pruned in One-Shot. In *International Conference on Machine Learning*, pages 10323–10337. PMLR.
- Elias Frantar, Saleh Ashkboos, Torsten Hoeffler, and Dan Alistarh. 2022. GPTQ: Accurate Post-Training Quantization for Generative Pre-trained Transformers. *arXiv preprint arXiv:2210.17323*.
- Leo Gao, Jonathan Tow, Baber Abbasi, Stella Biderman, Sid Black, Anthony DiPofi, Charles Foster, Laurence Golding, Jeffrey Hsu, Alain Le Noac’h, Haonan Li, Kyle McDonell, Niklas Muennighoff, Chris Ociepa, Jason Phang, Laria Reynolds, Hailey Schoelkopf, Aviya Skowron, Lintang Sutawika, and 5 others. 2024. [A framework for few-shot language model evaluation](#).
- Aaron Grattafiori, Abhimanyu Dubey, Abhinav Jauhri, Abhinav Pandey, Abhishek Kadian, Ahmad Al-Dahle, Aiesha Letman, Akhil Mathur, Alan Schelten, Alex Vaughan, and 1 others. 2024. The Llama 3 Herd of Models. *arXiv preprint arXiv:2407.21783*.
- Andrey Gromov, Kushal Tirumala, Hassan Shapourian, Paolo Glorioso, and Dan Roberts. 2025. [The Unreasonable Ineffectiveness of the Deeper Layers](#). In *International Conference on Learning Representations*.
- Yuto Harada, Yusuke Yamauchi, Yusuke Oda, Yohei Oseki, Yusuke Miyao, and Yu Takagi. 2025. [Massive Supervised Fine-tuning Experiments Reveal How Data, Layer, and Training Factors Shape LLM Alignment Quality](#). In *Proceedings of the 2025 Conference on Empirical Methods in Natural Language Processing*.
- Shwai He, Guoheng Sun, Zheyu Shen, and Ang Li. 2024. [What Matters in Transformers? Not All Attention is Needed](#). *Preprint*, arXiv:2406.15786.
- Dan Hendrycks, Collin Burns, Steven Basart, Andy Zou, Mantas Mazeika, Dawn Song, and Jacob Steinhardt. 2021. Measuring Massive Multitask Language Understanding. In *International Conference on Learning Representations*.
- Edward J Hu, Yelong Shen, Phillip Wallis, Zeyuan Allen-Zhu, Yuanzhi Li, Shean Wang, Lu Wang, and Weizhu Chen. 2022. [LoRA: Low-Rank Adaptation of Large Language Models](#). In *International Conference on Learning Representations*.
- Binyuan Hui, Jian Yang, Zeyu Cui, Jiayi Yang, Dayiheng Liu, Lei Zhang, Tianyu Liu, Jiajun Zhang, Bowen Yu, Keming Lu, and 1 others. 2024. Qwen2.5-Coder Technical Report. *arXiv preprint arXiv:2409.12186*.
- Yikun Jiang, Huanyu Wang, Tianhong Ding, Wenhu Zhang, Yiming Wu, Hanbin Zhao, and John C.S. Lui. 2026. [Equilibrium Language Models](#). In *International Conference on Learning Representations*.
- Sehoon Kim, Coleman Richard Charles Hooper, Amir Gholami, Zhen Dong, Xiuyu Li, Sheng Shen, Michael W. Mahoney, and Kurt Keutzer. 2024. [SqueezeLLM: Dense-and-Sparse Quantization](#). In *International Conference on Machine Learning*.
- Ji Lin, Jiaming Tang, Haotian Tang, Shang Yang, Weiming Chen, Wei-Chen Wang, Guangxuan Xiao, Xingyu Dang, Chuang Gan, and Song Han. 2024. AWQ: Activation-aware Weight Quantization for LLM Compression and Acceleration. *Proceedings of Machine Learning and Systems*, 6:87–100.
- Stephanie Lin, Jacob Hilton, and Owain Evans. 2022. TruthfulQA: Measuring How Models Mimic Human Falsehoods. In *Proceedings of the 60th Annual Meeting of the Association for Computational Linguistics (Volume 1: Long Papers)*, pages 3214–3252.
- Kainan Liu, Yong Zhang, Ning Cheng, Zhitao Li, Shaojun Wang, and Jing Xiao. 2025a. GRASP: Replace Redundant Layers with Adaptive Singular Parameters for Efficient Model Compression. In *Proceedings of the 2025 Conference on Empirical Methods in Natural Language Processing*, pages 26344–26359.
- Yijiang Liu, Huanrui Yang, Youxin Chen, Rongyu Zhang, Miao Wang, Yuan Du, and Li Du. 2025b. PAT: Pruning-Aware Tuning for Large Language Models. In *Proceedings of the AAAI Conference on Artificial Intelligence*, volume 39, pages 24686–24695.
- Zechun Liu, Barlas Oguz, Changsheng Zhao, Ernie Chang, Pierre Stock, Yashar Mehdad, Yangyang Shi, Raghuraman Krishnamoorthi, and Vikas Chandra. 2024. LLM-QAT: Data-Free Quantization Aware Training for Large Language Models. In *Findings of the Association for Computational Linguistics: ACL 2024*, pages 467–484.

- Xinyin Ma, Gongfan Fang, and Xinchao Wang. 2023. [LLM-Pruner: On the Structural Pruning of Large Language Models](#). In *Advances in Neural Information Processing Systems*.
- Xin Men, Mingyu Xu, Qingyu Zhang, Qianhao Yuan, Bingning Wang, Hongyu Lin, Yaojie Lu, Xianpei Han, and Weipeng Chen. 2025. ShortGPT: Layers in Large Language Models are More Redundant Than You Expect. In *Findings of the Association for Computational Linguistics: ACL 2025*, pages 20192–20204.
- Stephen Merity, Caiming Xiong, James Bradbury, and Richard Socher. 2016. Pointer Sentinel Mixture Models. *arXiv preprint arXiv:1609.07843*.
- Todor Mihaylov, Peter Clark, Tushar Khot, and Ashish Sabharwal. 2018. Can a Suit of Armor Conduct Electricity? A New Dataset for Open Book Question Answering. In *Proceedings of the 2018 Conference on Empirical Methods in Natural Language Processing*.
- Liana Mikaelyan, Ayyoob Imani, Mathew Salvaris, Parth Pathak, and Mohsen Fayyaz. 2025. [DeltaLLM: Compress LLMs with Low-Rank Deltas between Shared Weights](#). *Preprint*, arXiv:2501.18596.
- Subhabrata Mukherjee, Arindam Mitra, Ganesh Jawahar, Sahaj Agarwal, Hamid Palangi, and Ahmed Awadallah. 2023. Orca: Progressive Learning from Complex Explanation Traces of GPT-4. *CoRR*, abs/2306.02707.
- Denis Paperno, Germán Kruszewski, Angeliki Lazaridou, Ngoc Quan Pham, Raffaella Bernardi, Sandro Pezzelle, Marco Baroni, Gemma Boleda, and Raquel Fernández. 2016. [The LAMBADA dataset: Word prediction requiring a broad discourse context](#). In *Proceedings of the 54th Annual Meeting of the Association for Computational Linguistics (Volume 1: Long Papers)*, pages 1525–1534, Berlin, Germany. Association for Computational Linguistics.
- Colin Raffel, Noam Shazeer, Adam Roberts, Katherine Lee, Sharan Narang, Michael Matena, Yanqi Zhou, Wei Li, and Peter J. Liu. 2020. [Exploring the Limits of Transfer Learning with a Unified Text-to-Text Transformer](#). *Journal of Machine Learning Research*, 21(140):1–67.
- Anton Razzhigaev, Matvey Mikhalechuk, Elizaveta Goncharova, Nikolai Gerasimenko, Ivan Oseledets, Denis Dimitrov, and Andrey Kuznetsov. 2024. [Your Transformer is Secretly Linear](#). In *Proceedings of the 62nd Annual Meeting of the Association for Computational Linguistics (Volume 1: Long Papers)*, pages 5376–5384, Bangkok, Thailand. Association for Computational Linguistics.
- Keisuke Sakaguchi, Ronan Le Bras, Chandra Bhagavathula, and Yejin Choi. 2021. WinoGrande: an adversarial winograd schema challenge at scale. *Communications of the ACM*, 64(9):99–106.
- Fabrizio Sandri, Elia CuneGatti, and Giovanni Iacca. 2025. [2SSP: A Two-Stage Framework for Structured Pruning of LLMs](#). *Transactions on Machine Learning Research*.
- Maarten Sap, Hannah Rashkin, Derek Chen, Ronan Le Bras, and Yejin Choi. 2019. SocialIQA: Commonsense Reasoning about Social Interactions. In *Proceedings of the 2019 Conference on Empirical Methods in Natural Language Processing*.
- Melanie Sclar, Yejin Choi, Yulia Tsvetkov, and Alane Suhr. 2024. Quantifying Language Model’s Sensitivity to Spurious Features in Prompt Design or: How I learned to start worrying about prompt formatting. In *International Conference on Learning Representations*.
- Wenqi Shao, Mengzhao Chen, Zhaoyang Zhang, Peng Xu, Lirui Zhao, Zhiqian Li, Kaipeng Zhang, Gao Peng, Yu Qiao, and Ping Luo. 2024. OmniQuant: Omnidirectionally Calibrated Quantization for Large Language Models. In *International Conference on Learning Representations*, volume 2024, pages 45472–45496.
- Noam Shazeer. 2020. GLU Variants Improve Transformer. *arXiv preprint arXiv:2002.05202*.
- Zhiqiang Shen, Tianhua Tao, Liqun Ma, Willie Neiswanger, Zhengzhong Liu, Hongyi Wang, Bowen Tan, Joel Hestness, Natalia Vassilieva, Daria Soboleva, and Eric Xing. 2023. SlimPajama-DC: Understanding Data Combinations for LLM Training. *arXiv preprint arXiv:2309.10818*.
- Dmitriy Shopkhoev, Ammar Ali, Magauyiya Zhussip, Valentin Malykh, Stamatios Lefkimmiatis, Nikos Komodakis, and Sergey Zagoruyko. 2025. [ReplaceMe: Network Simplification via Depth Pruning and Transformer Block Linearization](#). In *Advances in Neural Information Processing Systems*, volume 38, pages 19487–19517. Curran Associates, Inc.
- Safal Shrestha, Anubhav Shrestha, Aadim Nepal, Minwu Kim, and Keith Ross. 2026. On the Limits of Layer Pruning for Generative Reasoning in LLMs. *arXiv preprint arXiv:2602.01997*.
- Shoaib Ahmed Siddiqui, Xin Dong, Greg Heinrich, Thomas Breuel, Jan Kautz, David Krueger, and Pavlo Molchanov. 2024. A deeper look at depth pruning of LLMs. In *ICML 2024 Workshop on Theoretical Foundations of Foundation Models*.
- Mingjie Sun, Zhuang Liu, Anna Bair, and Zico Kolter. 2024. [A Simple and Effective Pruning Approach for Large Language Models](#). In *International Conference on Learning Representations*, volume 2024, pages 4942–4964.
- Shengkun Tang, Oliver Sieberling, Eldar Kurtic, Zhiqiang Shen, and Dan Alistarh. 2025. DarwinLM: Evolutionary Structured Pruning of Large Language Models. *arXiv preprint arXiv:2502.07780*.

- Ashish Vaswani, Noam Shazeer, Niki Parmar, Jakob Uszkoreit, Llion Jones, Aidan N Gomez, Łukasz Kaiser, and Illia Polosukhin. 2017. [Attention is All you Need](#). In *Advances in Neural Information Processing Systems*, volume 30. Curran Associates, Inc.
- Johannes Welbl, Nelson F. Liu, and Matt Gardner. 2017. Crowdsourcing Multiple Choice Science Questions. In *Proceedings of the 3rd Workshop on Noisy User-generated Text*.
- Mengzhou Xia, Tianyu Gao, Zhiyuan Zeng, and Danqi Chen. 2024. Sheared LLaMA: Accelerating Language Model Pre-training via Structured Pruning. In *International Conference on Learning Representations*, volume 2024, pages 5385–5409.
- Guangxuan Xiao, Ji Lin, Mickael Seznec, Hao Wu, Julien Demouth, and Song Han. 2023. SmoothQuant: Accurate and Efficient Post-Training Quantization for Large Language Models. In *International Conference on Machine Learning*, pages 38087–38099. PMLR.
- An Yang, Anfeng Li, Baosong Yang, Beichen Zhang, Binyuan Hui, Bo Zheng, Bowen Yu, Chang Gao, Chengen Huang, Chenxu Lv, and 1 others. 2025. Qwen3 Technical Report. *arXiv preprint arXiv:2505.09388*.
- Yifei Yang, Zouying Cao, and Hai Zhao. 2024. LaCo: Large Language Model Pruning via Layer Collapse. In *Findings of the Association for Computational Linguistics: EMNLP 2024*, pages 6401–6417.
- Rowan Zellers, Ari Holtzman, Yonatan Bisk, Ali Farhadi, and Yejin Choi. 2019. HellaSwag: Can a Machine Really Finish Your Sentence? In *Proceedings of the 57th Annual Meeting of the Association for Computational Linguistics*.
- Longguang Zhong, Fanqi Wan, Ruijun Chen, Xiaojun Quan, and Liangzhi Li. 2025. [BlockPruner: Fine-grained Pruning for Large Language Models](#). In *Findings of the Association for Computational Linguistics: ACL 2025*, pages 5065–5080, Vienna, Austria. Association for Computational Linguistics.

## A Appendix

### A.1 Additional base-model perplexity results

Tables A1 and A2 report the remaining base-model perplexity results at 20%, 30%, and 37.5% sparsity. These results complement the main language-modeling table, which reports 12.5% and 25%. Overall, the additional sparsities show the same trend as the main results: SUBFIT usually provides the lowest PPL degradation, especially as sparsity increases. The main exceptions are Qwen3-8B and DeepSeek-7B at some sparsity levels, where the strongest baseline remains competitive or slightly better. This is consistent with the results reported in the main text: SUBFIT improves the aggregate trade-off, but does not dominate every individual model-sparsity setting.

Table A1: Perplexity comparison at representative sparsity levels. Lower PPL is better; PPL Deg. is the geometric mean of sparse/dense PPL ratios.

Sparsity	Method	Lambada ↓	C4 ↓	WikiText2 ↓	PPL Deg. ↓
<b>Qwen3-8B</b>					
Dense		25.70	15.25	9.72	1.00×
20%	Streamline (FFN)	<b>45.75</b>	<b>27.01</b>	<b>24.48</b>	<b>1.99×</b>
	Streamline (Layer)	61.51	41.29	57.08	3.36×
	ReplaceMe (LS)	77.52	58.55	101.88	4.95×
	ReplaceMe (Cosine)	66.91	46.79	68.68	3.84×
	<b>SUBFIT</b>	<b>50.25</b>	<b>30.69</b>	<b>28.01</b>	<b>2.25×</b>
30%	Streamline (FFN)	129.13	91.62	140.29	7.58×
	Streamline (Layer)	138.22	83.89	123.24	7.21×
	ReplaceMe (LS)	189.33	192.84	498.45	16.84×
	ReplaceMe (Cosine)	85.49	<b>50.95</b>	<b>58.54</b>	<b>4.06×</b>
	<b>SUBFIT</b>	<b>78.61</b>	52.22	64.53	4.11×
37.5%	Streamline (FFN)	444.17	387.86	737.90	32.19×
	Streamline (Layer)	392.86	288.44	497.86	24.55×
	ReplaceMe (LS)	168.22	118.58	261.60	11.10×
	ReplaceMe (Cosine)	<b>124.01</b>	<b>82.56</b>	<b>106.55</b>	<b>6.59×</b>
	<b>SUBFIT</b>	129.88	103.97	174.30	8.52×
<b>DeepSeek-7B</b>					
Dense		14.36	9.75	6.85	1.00×
20%	Streamline (FFN)	25.33	20.43	17.14	2.10×
	Streamline (Layer)	25.55	20.32	17.39	2.11×
	ReplaceMe (LS)	23.42	18.87	15.59	1.93×
	ReplaceMe (Cosine)	<b>21.67</b>	18.21	13.87	1.79×
	<b>SUBFIT</b>	25.22	<b>15.53</b>	<b>12.38</b>	<b>1.72×</b>
30%	Streamline (FFN)	57.44	66.55	90.21	7.11×
	Streamline (Layer)	43.40	47.06	60.41	5.05×
	ReplaceMe (LS)	40.28	41.42	44.68	4.27×
	ReplaceMe (Cosine)	53.75	49.66	61.55	5.55×
	<b>SUBFIT</b>	<b>36.51</b>	<b>26.96</b>	<b>27.33</b>	<b>3.04×</b>
37.5%	Streamline (FFN)	64.56	65.22	103.33	7.68×
	Streamline (Layer)	<b>42.70</b>	<b>39.00</b>	58.96	<b>4.68×</b>
	ReplaceMe (LS)	60.16	72.76	78.37	7.10×
	ReplaceMe (Cosine)	119.19	111.82	140.86	12.51×
	<b>SUBFIT</b>	50.90	43.52	<b>46.13</b>	4.74×

### A.2 Additional instruction-tuned downstream results

Tables A3 to A6 report task-level instruction-tuned results at the remaining sparsity levels. These tables provide the per-task breakdown behind the

Table A2: Perplexity comparison at representative sparsity levels. Lower PPL is better; PPL Deg. is the geometric mean of sparse/dense PPL ratios.

Sparsity	Method	Lambada ↓	C4 ↓	WikiText2 ↓	PPL Deg. ↓
<b>Llama-3.2-3B</b>					
Dense		20.15	11.07	7.82	1.00×
20%	Streamline (FFN)	43.68	27.35	20.47	2.41×
	Streamline (Layer)	38.15	25.80	25.05	2.42×
	ReplaceMe (LS)	42.61	27.13	27.83	2.64×
	ReplaceMe (Cosine)	43.74	28.39	27.37	2.69×
	<b>SUBFIT</b>	<b>31.94</b>	<b>19.06</b>	<b>13.84</b>	<b>1.69×</b>
30%	Streamline (FFN)	65.94	43.51	54.44	4.47×
	Streamline (Layer)	55.31	41.39	49.86	4.03×
	ReplaceMe (LS)	66.21	44.22	51.57	4.42×
	ReplaceMe (Cosine)	67.11	45.64	50.56	4.46×
	<b>SUBFIT</b>	<b>49.67</b>	<b>26.23</b>	<b>24.35</b>	<b>2.63×</b>
37.5%	Streamline (FFN)	129.14	86.77	134.00	9.51×
	Streamline (Layer)	108.99	74.83	105.90	7.91×
	ReplaceMe (LS)	94.43	64.26	94.53	6.90×
	ReplaceMe (Cosine)	108.02	72.42	104.68	7.77×
	<b>SUBFIT</b>	<b>75.27</b>	<b>45.02</b>	<b>58.62</b>	<b>4.85×</b>
<b>Qwen3-4B</b>					
Dense		33.80	19.89	13.67	1.00×
20%	Streamline (FFN)	95.64	63.30	88.98	3.88×
	Streamline (Layer)	78.93	52.93	71.06	3.18×
	ReplaceMe (LS)	94.79	61.99	83.00	3.76×
	ReplaceMe (Cosine)	74.98	49.95	48.77	2.71×
	<b>SUBFIT</b>	<b>54.36</b>	<b>32.63</b>	<b>30.01</b>	<b>1.80×</b>
30%	Streamline (FFN)	273.13	212.23	377.12	13.35×
	Streamline (Layer)	323.62	275.06	546.83	17.43×
	ReplaceMe (LS)	261.67	286.36	597.41	16.95×
	ReplaceMe (Cosine)	440.84	522.68	642.38	25.25×
	<b>SUBFIT</b>	<b>92.19</b>	<b>58.99</b>	<b>72.37</b>	<b>3.50×</b>
37.5%	Streamline (FFN)	721.51	726.79	1344.13	42.49×
	Streamline (Layer)	718.56	662.92	1187.55	39.48×
	ReplaceMe (LS)	522.03	552.81	1206.99	33.59×
	ReplaceMe (Cosine)	5394.41	6397.86	10402.30	339.31×
	<b>SUBFIT</b>	<b>124.51</b>	<b>99.91</b>	<b>140.65</b>	<b>5.75×</b>
<b>Llama-3.1-8B</b>					
Dense		17.78	9.36	6.24	1.00×
20%	Streamline (FFN)	28.55	19.58	18.39	2.15×
	Streamline (Layer)	<b>25.79</b>	18.26	12.51	1.78×
	ReplaceMe (LS)	28.16	18.28	13.40	1.88×
	ReplaceMe (Cosine)	26.59	18.29	12.68	1.81×
	<b>SUBFIT</b>	28.04	<b>15.60</b>	<b>10.90</b>	<b>1.66×</b>
30%	Streamline (FFN)	58.06	44.45	65.27	5.45×
	Streamline (Layer)	49.86	44.68	56.65	4.95×
	ReplaceMe (LS)	68.58	54.84	73.81	6.44×
	ReplaceMe (Cosine)	99.62	73.21	90.50	8.60×
	<b>SUBFIT</b>	<b>44.05</b>	<b>27.27</b>	<b>23.40</b>	<b>3.00×</b>
37.5%	Streamline (FFN)	98.14	78.12	157.99	10.52×
	Streamline (Layer)	81.19	71.12	102.69	8.29×
	ReplaceMe (LS)	109.84	84.32	140.14	10.77×
	ReplaceMe (Cosine)	346.09	152.17	317.25	25.24×
	<b>SUBFIT</b>	<b>69.11</b>	<b>43.69</b>	<b>62.07</b>	<b>5.65×</b>

aggregate retention values in Table 3. Across sparsities, SUBFIT generally preserves the strongest downstream average, while some individual tasks and models remain better served by specific baselines.

### A.3 Calibration sensitivity

Figure A1 varies the number of calibration samples used to fit the replacement modules. SUBFIT is stable across calibration budgets, with limited changes beyond 2k–4k samples for both base-model PPL and instruction-tuned accuracy. This suggests that

Table A3: Downstream performance (%) at sparsity 12.5%. Acc. Ret. is the ratio sparse/dense aggregate accuracy.

Model	Sparsity	Commonsense					QA		Knowledge	Reasoning		Math	Science	Average	
		HS	PIQA	Wino	OBQA	SIQA	BoolQ	TQA	MMLU	ARC-C	ARC-E	MathQA	SciQ	Avg	Acc. Ret.
<b>Llama-3.2-3B-Instruct</b>	Dense	64.53	75.63	67.88	42.00	46.11	75.63	33.54	61.84	45.31	68.10	26.03	87.90	57.87	100.00%
Streamline (FFN)		59.91	<b>71.16</b>	67.40	35.00	<b>45.80</b>	74.19	<b>31.58</b>	50.03	39.42	59.68	23.82	83.40	53.45	92.36%
Streamline (Layer)		<b>60.16</b>	70.40	65.90	35.00	45.29	75.29	31.46	56.20	38.57	59.81	<b>24.46</b>	86.00	54.04	93.38%
ReplaceMe (LS)	12.5%	58.32	70.40	<b>68.51</b>	<b>36.40</b>	44.73	<b>80.18</b>	30.60	<b>61.65</b>	37.88	57.66	23.79	81.70	54.32	93.86%
ReplaceMe (Cosine)		58.94	70.40	<b>68.51</b>	36.00	44.58	79.57	30.48	61.51	38.65	58.80	23.85	83.60	54.57	94.30%
SUBFIT		58.88	69.15	68.11	35.20	45.24	79.88	29.99	61.07	<b>39.51</b>	<b>60.23</b>	23.08	<b>89.40</b>	<b>54.98</b>	<b>95.00%</b>
<b>Qwen3-4B-Instruct</b>	Dense	43.42	69.70	56.75	40.80	46.32	84.83	39.17	72.18	43.17	55.43	33.30	67.50	54.38	100.00%
Streamline (FFN)		39.39	63.22	58.48	34.80	40.89	83.52	38.80	71.24	36.95	43.14	28.27	62.90	50.13	92.19%
Streamline (Layer)		40.50	65.56	<b>59.43</b>	36.60	42.58	83.61	<b>39.78</b>	71.41	37.88	48.19	28.04	63.40	<b>51.42</b>	<b>94.55%</b>
ReplaceMe (LS)	12.5%	<b>44.49</b>	<b>70.46</b>	56.04	39.00	43.96	73.46	31.70	47.48	<b>41.72</b>	<b>56.06</b>	27.47	<b>72.30</b>	50.34	92.58%
ReplaceMe (Cosine)		44.38	70.24	54.46	<b>39.80</b>	<b>44.32</b>	75.87	32.68	49.57	40.36	55.60	28.48	68.50	50.35	92.60%
SUBFIT		36.05	62.24	58.17	37.20	43.14	<b>85.72</b>	<b>39.78</b>	<b>72.08</b>	34.73	44.65	<b>29.08</b>	63.70	50.55	92.95%
<b>Qwen2.5-7B-Instruct</b>	Dense	65.48	73.50	61.01	44.00	45.75	85.81	47.49	73.51	43.34	50.84	34.17	55.40	56.69	100.00%
Streamline (FFN)		<b>60.88</b>	<b>75.14</b>	59.04	39.40	42.58	71.65	28.03	40.08	38.40	44.15	30.28	<b>55.20</b>	48.74	85.97%
Streamline (Layer)		60.57	74.81	61.64	42.20	43.04	75.11	28.15	47.42	38.91	46.51	30.89	54.70	50.33	88.77%
ReplaceMe (LS)	12.5%	60.26	71.87	<b>62.43</b>	<b>43.00</b>	44.47	75.54	32.44	49.41	39.42	<b>47.26</b>	30.92	51.40	<b>50.70</b>	<b>89.43%</b>
ReplaceMe (Cosine)		58.93	72.96	61.80	42.40	<b>44.78</b>	72.42	31.58	49.42	<b>40.10</b>	46.76	<b>31.22</b>	51.80	50.35	88.81%
SUBFIT		56.11	72.96	58.01	41.60	43.09	<b>81.01</b>	<b>34.76</b>	<b>51.05</b>	36.86	46.13	29.82	49.60	50.08	88.34%
<b>DeepSeek-7B-chat</b>	Dense	70.56	77.64	74.90	44.80	50.46	83.98	37.21	50.90	41.55	62.63	27.54	78.40	58.38	100.00%
Streamline (FFN)		63.66	73.83	72.69	39.80	47.39	83.12	32.93	51.05	38.91	55.30	25.36	67.40	54.29	92.99%
Streamline (Layer)		63.35	73.61	73.24	39.80	47.39	84.04	<b>33.90</b>	51.13	37.80	56.02	26.87	70.80	54.83	93.92%
ReplaceMe (LS)	12.5%	61.79	73.61	73.80	40.00	<b>47.95</b>	83.70	33.41	50.80	37.88	54.29	27.00	67.20	54.29	92.99%
ReplaceMe (Cosine)		<b>63.87</b>	<b>73.88</b>	<b>73.95</b>	41.20	47.59	80.73	32.80	50.73	<b>39.68</b>	<b>58.71</b>	26.63	<b>77.40</b>	<b>55.60</b>	<b>95.24%</b>
SUBFIT		62.89	73.45	73.80	<b>41.40</b>	<b>47.95</b>	<b>84.37</b>	33.54	<b>51.32</b>	38.91	56.69	<b>27.27</b>	73.50	55.42	94.94%
<b>Llama-3.1-8B-Instruct</b>	Dense	72.52	79.49	77.82	49.00	50.20	83.88	40.39	68.79	53.58	75.76	26.80	91.70	64.16	100.00%
Streamline (FFN)		<b>70.12</b>	76.71	<b>77.11</b>	44.80	<b>49.39</b>	73.33	36.35	67.76	49.06	72.90	25.09	<b>90.60</b>	61.10	95.23%
Streamline (Layer)		69.60	76.88	<b>77.11</b>	<b>45.80</b>	49.23	70.73	37.21	67.90	48.98	<b>73.70</b>	26.03	90.50	61.14	95.29%
ReplaceMe (LS)	12.5%	68.24	<b>77.04</b>	76.40	45.20	48.67	73.03	37.45	68.16	48.38	72.64	25.70	88.50	60.78	94.74%
ReplaceMe (Cosine)		68.70	76.55	76.32	45.20	49.33	72.32	<b>38.43</b>	<b>68.29</b>	<b>49.32</b>	73.02	25.49	89.50	61.04	95.14%
SUBFIT		68.19	76.39	75.37	45.40	49.33	<b>80.89</b>	37.45	66.65	48.63	72.69	<b>26.10</b>	89.70	<b>61.40</b>	<b>95.70%</b>

the fitted residual replacements do not require a large calibration set, making SUBFIT practical in low-data regimes.

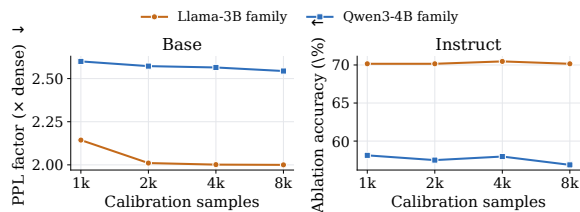


Figure A1: Calibration data sensitivity at 25% sparsity.

#### A.4 GSM8K

Table A7 reports GSM8K accuracy for all instruction-tuned models and sparsity levels. The results show large variation across methods, especially at low and moderate sparsity, and many compressed models collapse to very low GSM8K accuracy at higher sparsity. This supports our decision to report GSM8K separately rather than include it in the main downstream aggregate (see Section 6).

#### A.5 Offline runtime

Table A8 reports the average runtime of the post-training compression and evaluation pipeline. These values include selection, fitting, and evalua-

tion, and should therefore be interpreted as offline compression cost rather than deployed inference latency. SUBFIT is slower than simpler pruning baselines in this stage because it performs sequential selection and closed-form residual fitting for both Attention and FFN replacements.

#### A.6 Deployed parameter and MAC accounting

Table A9 and Table A10 provide detailed deployed-cost accounting. The added parameters correspond to stored replacement modules after compression. For SUBFIT, Attention and FFN compensation are reported separately; the shared FFN basis is counted once per model. ReplaceMe has zero added deployed parameters because its fitted transformation is folded into an existing projection. MACs are theoretical estimates for one forward pass with sequence length 2048 and are reported separately from offline runtime.

## B Evaluation Tasks

**Perplexity datasets (base models).** We evaluate perplexity on three standard benchmarks covering complementary text domains: Lambada Paperno et al., 2016 for narrative text, C4 Raffel et al., 2020 for web text, and WikiText-2 Merity et al., 2016 for encyclopedic text.

Table A4: Downstream performance (%) at sparsity 20%. Acc. Ret. is the ratio sparse/dense aggregate accuracy.

Model	Sparsity	Commonsense					QA		Knowledge	Reasoning		Math	Science	Average	
		HS	PIQA	Wino	OBQA	SIQA	BoolQ	TQA	MMLU	ARC-C	ARC-E	MathQA	SciQ	Avg	Acc. Ret.
<b>Llama-3.2-3B-Instruct</b>	Dense	64.53	75.63	67.88	42.00	46.11	75.63	33.54	61.84	45.31	68.10	26.03	87.90	57.87	100.00%
Streamline (FFN)		53.44	66.87	<b>67.96</b>	32.00	42.07	80.12	28.40	60.02	34.39	51.30	<b>23.69</b>	72.00	51.02	88.16%
Streamline (Layer)		54.83	66.05	66.30	32.80	42.94	62.69	30.72	35.39	36.43	53.24	23.35	74.90	48.30	83.46%
ReplaceMe (LS)	20%	51.97	66.27	66.22	32.80	42.73	80.92	30.97	61.28	33.87	50.08	23.05	72.60	51.06	88.23%
ReplaceMe (Cosine)		53.30	66.38	67.40	33.20	42.02	<b>81.71</b>	30.97	<b>61.47</b>	33.87	50.25	22.88	73.40	51.40	88.82%
SUBFIT		<b>55.03</b>	<b>67.85</b>	65.35	<b>35.20</b>	<b>44.32</b>	71.77	<b>31.21</b>	61.00	<b>37.46</b>	<b>56.48</b>	22.68	<b>81.70</b>	<b>52.50</b>	<b>90.72%</b>
<b>Qwen3-4B-Instruct</b>	Dense	43.42	69.70	56.75	40.80	46.32	84.83	39.17	72.18	43.17	55.43	33.30	67.50	54.38	100.00%
Streamline (FFN)		32.02	54.62	55.64	31.40	37.72	<b>83.64</b>	32.19	<b>71.51</b>	29.18	35.35	25.93	57.70	45.58	83.81%
Streamline (Layer)		32.51	56.64	<b>57.22</b>	33.00	38.69	73.58	34.64	71.02	30.46	37.84	<b>26.73</b>	55.70	45.67	83.98%
ReplaceMe (LS)	20%	<b>40.13</b>	68.17	52.96	<b>36.40</b>	40.07	57.92	31.21	32.59	<b>35.07</b>	<b>45.75</b>	24.99	55.00	43.36	79.73%
ReplaceMe (Cosine)		40.07	<b>68.72</b>	53.59	35.40	<b>41.66</b>	62.54	30.60	34.57	34.47	45.37	26.13	52.90	43.83	80.61%
SUBFIT		30.69	56.64	55.80	34.20	41.50	72.20	<b>36.72</b>	70.51	29.95	38.30	<b>26.73</b>	<b>62.30</b>	<b>46.30</b>	<b>85.13%</b>
<b>Qwen2.5-7B-Instruct</b>	Dense	65.48	73.50	61.01	44.00	45.75	85.81	47.49	73.51	43.34	50.84	34.17	55.40	56.69	100.00%
Streamline (FFN)		55.27	71.76	55.80	39.80	41.30	60.49	26.07	30.16	33.87	42.21	29.15	52.60	44.87	79.15%
Streamline (Layer)		<b>56.51</b>	73.18	55.25	40.80	42.17	65.84	26.19	31.67	34.30	44.78	28.54	54.30	46.13	81.37%
ReplaceMe (LS)	20%	55.88	72.80	55.17	39.60	42.27	66.70	29.38	32.59	<b>37.88</b>	45.41	29.31	<b>54.50</b>	46.79	82.53%
ReplaceMe (Cosine)		56.34	<b>73.23</b>	57.38	<b>42.40</b>	<b>43.65</b>	65.87	29.50	34.03	37.03	<b>45.96</b>	<b>29.75</b>	53.90	<b>47.42</b>	<b>83.65%</b>
SUBFIT		51.49	71.38	<b>57.70</b>	40.00	41.04	<b>69.45</b>	<b>33.41</b>	<b>39.45</b>	35.07	44.40	28.64	52.30	47.03	82.95%
<b>DeepSeek-7B-chat</b>	Dense	70.56	77.64	74.90	44.80	50.46	83.98	37.21	50.90	41.55	62.63	27.54	78.40	58.38	100.00%
Streamline (FFN)		<b>60.70</b>	70.40	74.35	35.60	46.01	77.49	31.82	48.40	36.18	50.34	22.75	62.90	51.41	88.06%
Streamline (Layer)		56.61	68.50	73.64	35.80	46.11	78.65	<b>32.44</b>	49.88	34.56	49.41	22.61	61.50	50.81	87.03%
ReplaceMe (LS)	20%	55.15	69.04	<b>74.43</b>	37.60	46.32	78.93	31.82	50.48	34.04	49.83	23.85	59.70	50.93	87.24%
ReplaceMe (Cosine)		59.55	<b>70.57</b>	73.09	35.60	46.37	79.54	<b>32.44</b>	46.76	<b>36.69</b>	<b>53.24</b>	24.59	<b>73.60</b>	<b>52.67</b>	<b>90.22%</b>
SUBFIT		55.21	69.80	71.03	<b>40.00</b>	<b>46.98</b>	<b>84.28</b>	<b>32.44</b>	<b>50.75</b>	35.75	52.99	<b>24.82</b>	67.20	<b>52.60</b>	<b>90.11%</b>
<b>Llama-3.1-8B-Instruct</b>	Dense	72.52	79.49	77.82	49.00	50.20	83.88	40.39	68.79	53.58	75.76	26.80	91.70	64.16	100.00%
Streamline (FFN)		<b>66.37</b>	<b>74.43</b>	75.22	40.20	47.59	80.58	35.62	67.60	43.17	<b>65.82</b>	23.38	85.10	<b>58.76</b>	<b>91.58%</b>
Streamline (Layer)		65.82	74.27	74.82	39.60	<b>48.16</b>	77.31	35.99	67.72	<b>43.52</b>	65.45	23.42	<b>86.90</b>	58.58	91.30%
ReplaceMe (LS)	20%	63.56	72.42	74.82	42.00	45.91	81.47	36.60	<b>68.24</b>	43.26	65.74	<b>25.03</b>	85.10	58.68	91.45%
ReplaceMe (Cosine)		65.71	73.67	74.51	41.00	47.29	75.66	<b>37.33</b>	68.02	42.58	64.90	24.05	83.70	58.20	90.71%
SUBFIT		63.41	72.09	<b>75.61</b>	<b>42.20</b>	46.93	<b>83.33</b>	34.76	67.59	41.72	65.61	24.56	86.20	58.67	91.44%

### Downstream tasks (instruction-tuned models).

We evaluate on thirteen downstream tasks grouped by capability. *Commonsense reasoning*: HelLaSwag (Zellers et al., 2019), PIQA (Bisk et al., 2020), Winogrande (Sakaguchi et al., 2021), OpenBookQA (Mihaylov et al., 2018), SocialIQA (Sap et al., 2019). *Question answering*: BoolQ (Clark et al., 2019), TruthfulQA (Lin et al., 2022). *Knowledge*: MMLU (Hendrycks et al., 2021). *Reasoning*: ARC-Challenge and ARC-Easy (Clark et al., 2018). *Math*: MathQA (Amini et al., 2019), GSM8K (Cobbe et al., 2021). *Science*: SciQ (Welbl et al., 2017). All tasks have been evaluated using a zero-shot setup apart from Winogrande, MMLU, and GSM8K, which have been evaluated in a five-shot scenario.

**Ablation subset.** The ablation studies in Section 5 use a reduced zero-shot subset of five tasks: PIQA, Winogrande, ARC-Easy, BoolQ, and SciQ. All tasks use the LM Evaluation Harness (Gao et al., 2024).

## C Experimental Setup Details

**Models.** We evaluate SUBFIT on ten LLMs spanning three families and the 3B–8B scale. The five base models are Llama-3.2-3B (Grattafiori et al., 2024), Qwen3-4B (Yang et al., 2025), Llama-3.1-8B (Grattafiori et al., 2024), Qwen3-

8B (Yang et al., 2025), and DeepSeek-7B (Bi et al., 2024). The five instruction-tuned models are Llama-3.2-3B-Instruct (Grattafiori et al., 2024), Qwen3-4B-Instruct (Yang et al., 2025), Qwen2.5-7B-Instruct (Hui et al., 2024), Llama-3.1-8B-Instruct (Grattafiori et al., 2024), and DeepSeek-7B-chat (Bi et al., 2024). All models are loaded from the HuggingFace Hub using their public checkpoints; we operate on the full-precision (bf16) weights and do not apply quantization at any stage of compression or evaluation.

**Sparsity grid.** We evaluate at five sparsity levels: 12.5%, 20%, 25%, 30%, and 37.5%. For a model with  $L$  Transformer layers and target sparsity  $s$ , SUBFIT selects  $\text{round}(L \cdot s)$  Attention submodules and the same number of FFN submodules; the baselines remove  $\text{round}(L \cdot s)$  full Transformer layers, matching the overall parameter budget.

**Evaluation tasks.** For base models, we report perplexity on Lambada, C4, and WikiText-2, and summarize each model with the *PPL factor*, defined as the geometric mean of sparse-to-dense PPL ratios across the three datasets, as done in (Cunegatti et al., 2025). For instruction-tuned models, we report zero/few-shot accuracy on thirteen downstream tasks grouped into six categories: commonsense reasoning, question answering, knowledge, reasoning, math, and science. The complete task

Table A5: Downstream performance (%) at sparsity 30%. Acc. Ret. is the ratio sparse/dense aggregate accuracy.

Model	Sparsity	Commonsense					QA		Knowledge	Reasoning		Math	Science	Average	
		HS	PIQA	Wino	OBQA	SIQA	BoolQ	TQA	MMLU	ARC-C	ARC-E	MathQA	SciQ	Avg	Acc. Ret.
<b>Llama-3.2-3B-Instruct</b>	Dense	64.53	75.63	67.88	42.00	46.11	75.63	33.54	61.84	45.31	68.10	26.03	87.90	57.87	100.00%
Streamline (FFN)		46.77	64.04	65.19	32.60	40.48	78.56	28.27	41.51	32.51	43.69	21.07	65.70	46.70	80.69%
Streamline (Layer)		48.55	<b>64.25</b>	<b>65.51</b>	32.40	41.20	77.46	27.66	41.60	<b>33.53</b>	46.00	21.14	69.60	47.41	81.92%
ReplaceMe (LS)	30%	47.74	63.06	60.93	33.80	40.48	<b>79.33</b>	28.27	<b>60.36</b>	31.06	46.68	22.35	68.40	48.54	83.87%
ReplaceMe (Cosine)		<b>50.17</b>	63.77	60.85	<b>34.00</b>	40.89	76.18	29.99	56.16	32.08	<b>47.73</b>	<b>23.35</b>	70.60	48.81	84.34%
SUBFIT		48.51	63.44	64.64	32.00	<b>41.61</b>	78.99	<b>30.60</b>	60.16	32.94	47.14	21.84	<b>75.70</b>	<b>49.80</b>	<b>86.04%</b>
<b>Qwen3-4B-Instruct</b>	Dense	43.42	69.70	56.75	40.80	46.32	84.83	39.17	72.18	43.17	55.43	33.30	67.50	54.38	100.00%
Streamline (FFN)		23.69	51.58	51.62	32.40	34.85	<b>68.87</b>	24.85	22.94	25.60	30.13	20.47	21.80	34.07	62.64%
Streamline (Layer)		22.51	48.53	51.38	33.60	34.44	63.52	25.70	27.29	25.00	28.16	21.81	20.60	33.54	61.69%
ReplaceMe (LS)	30%	33.94	<b>63.82</b>	53.04	<b>34.20</b>	36.85	44.92	37.70	26.42	<b>29.44</b>	<b>39.27</b>	<b>24.36</b>	51.90	39.65	72.92%
ReplaceMe (Cosine)		<b>35.06</b>	62.02	50.99	33.60	38.02	56.73	<b>38.07</b>	26.93	29.10	36.03	23.48	53.70	40.31	74.13%
SUBFIT		28.71	54.57	<b>55.25</b>	33.60	<b>39.10</b>	65.20	33.41	<b>56.30</b>	27.39	35.10	24.19	<b>54.80</b>	<b>42.30</b>	<b>77.79%</b>
<b>Qwen2.5-7B-Instruct</b>	Dense	65.48	73.50	61.01	44.00	45.75	85.81	47.49	73.51	43.34	50.84	34.17	55.40	56.69	100.00%
Streamline (FFN)		49.67	71.55	51.78	39.40	40.12	62.17	24.11	26.79	32.25	43.01	25.90	<b>57.80</b>	43.71	77.11%
Streamline (Layer)		50.49	<b>72.09</b>	53.28	38.60	39.92	62.17	23.99	26.73	32.85	43.10	26.03	55.90	43.76	77.19%
ReplaceMe (LS)	30%	50.50	68.99	56.20	39.40	42.43	62.14	29.99	28.98	34.13	42.00	<b>27.77</b>	49.90	44.37	78.26%
ReplaceMe (Cosine)		<b>50.82</b>	70.19	<b>58.64</b>	<b>40.60</b>	<b>42.94</b>	63.27	30.35	29.24	<b>34.22</b>	<b>44.07</b>	27.64	55.20	<b>45.60</b>	<b>80.43%</b>
SUBFIT		45.65	68.77	54.14	39.00	40.58	<b>66.57</b>	<b>30.97</b>	<b>33.13</b>	32.51	41.54	26.00	51.00	44.16	77.89%
<b>DeepSeek-7B-chat</b>	Dense	70.56	77.64	74.90	44.80	50.46	83.98	37.21	50.90	41.55	62.63	27.54	78.40	58.38	100.00%
Streamline (FFN)		26.71	54.73	61.56	28.80	36.49	63.36	27.05	29.50	29.69	32.74	18.86	30.60	36.68	62.82%
Streamline (Layer)		46.52	64.15	69.22	<b>34.80</b>	40.43	63.27	25.21	<b>45.25</b>	28.84	39.52	22.85	42.90	43.58	74.65%
ReplaceMe (LS)	30%	42.85	60.28	68.11	33.60	40.69	67.09	26.81	40.31	29.01	37.92	22.38	34.60	41.97	71.89%
ReplaceMe (Cosine)		<b>47.81</b>	<b>70.84</b>	53.20	33.80	40.43	53.52	26.68	25.59	26.37	<b>47.98</b>	23.58	<b>73.90</b>	43.64	74.75%
SUBFIT		44.78	62.24	<b>70.01</b>	31.80	<b>43.76</b>	<b>79.45</b>	<b>28.15</b>	37.69	<b>29.95</b>	41.92	<b>23.99</b>	49.40	<b>45.26</b>	<b>77.53%</b>
<b>Llama-3.1-8B-Instruct</b>	Dense	72.52	79.49	77.82	49.00	50.20	83.88	40.39	68.79	53.58	75.76	26.80	91.70	64.16	100.00%
Streamline (FFN)		49.18	62.79	72.14	32.00	41.25	82.35	32.80	62.19	33.53	44.32	21.04	69.60	50.27	78.34%
Streamline (Layer)		49.41	63.00	71.35	32.60	41.81	81.90	31.21	62.28	35.49	47.10	21.68	70.40	50.69	79.00%
ReplaceMe (LS)	30%	50.92	64.09	71.11	34.80	41.35	84.04	33.41	<b>67.18</b>	33.62	49.71	21.54	75.10	52.24	81.42%
ReplaceMe (Cosine)		53.18	65.94	71.51	<b>36.20</b>	42.68	84.22	<b>36.60</b>	66.42	34.47	46.55	22.08	71.90	52.64	82.05%
SUBFIT		<b>54.26</b>	<b>67.14</b>	<b>72.53</b>	35.40	<b>43.40</b>	<b>84.25</b>	34.27	66.63	<b>36.26</b>	<b>53.20</b>	<b>22.88</b>	<b>82.20</b>	<b>54.37</b>	<b>84.74%</b>

list with dataset references is in Section B. All downstream evaluations are run with the LM Evaluation Harness (Gao et al., 2024) under identical conditions across methods.

**Baselines.** We compare against four block-replacement baselines that match SUBFIT’s post-training, calibration-only replacement setting. **Streamline (FFN)** (Chen et al., 2025b) selects a contiguous range of layers by cosine similarity between input and output residual states and replaces the block with a trained feed-forward network. **Streamline (Layer)** (Chen et al., 2025b) uses the same selection but substitutes the removed block with a full Transformer layer (self-attention plus feed-forward). **ReplaceMe (LS)** (Shopkhoev et al., 2025) and **ReplaceMe (Cosine)** (Shopkhoev et al., 2025) both fit a single linear transformation for the contiguous removed block, folded into the preceding layer’s projection at deployment, so no parameters are added at inference; the two variants differ in the criterion used to identify the contiguous range, least-squares reconstruction error (LS) or cosine similarity (Cosine).

**Choice of baselines.** Our primary baselines are LLM-Streamline (Chen et al., 2025b) and ReplaceMe (Shopkhoev et al., 2025), because they match the setting studied in this paper: post-training replacement of removed Transformer com-

ponents using calibration data, with a deployable compressed model. LLM-Streamline removes a contiguous sequence of layers and trains a lightweight replacement module to recover the lost computation; we include both its FeedForward replacement and full layer replacement variants. ReplaceMe removes a contiguous block of Transformer layers and fits a single linear map from calibration activations, which can be folded into adjacent weights at deployment; we include both its least-squares and cosine-based selection variants. These four baselines therefore share the two design constraints relaxed by SUBFIT: full-layer granularity and contiguous selection, while remaining in the same post-training, calibration-based replacement setting.

We do not include LinearPatch (Chen et al., 2026a), GRASP (Liu et al., 2025a), or ELM (Jiang et al., 2026) as main baselines because they target related but different recovery settings, even though we include them in the related work. Specifically, LinearPatch starts from an already-layer-pruned model and inserts a lightweight linear correction between the remaining blocks to reduce activation-magnitude mismatch; it does not jointly select and replace submodules from the dense model. GRASP is a layer-level hybrid pruning method: it identifies redundant layers and retains sensitivity-aware

Table A6: Downstream performance (%) at sparsity 37.5%. Acc. Ret. is the ratio sparse/dense aggregate accuracy.

Model	Sparsity	Commonsense					QA		Knowledge	Reasoning		Math	Science	Average	
		HS	PIQA	Wino	OBQA	SIQA	BoolQ	TQA	MMLU	ARC-C	ARC-E	MathQA	SciQ	Avg	Acc. Ret.
<b>Llama-3.2-3B-Instruct</b>	Dense	64.53	75.63	67.88	42.00	46.11	75.63	33.54	61.84	45.31	68.10	26.03	87.90	57.87	100.00%
Streamline (FFN)		42.20	60.39	<b>64.48</b>	31.00	38.79	<b>76.64</b>	27.42	48.68	31.23	38.64	20.34	29.20	42.42	73.29%
Streamline (Layer)		<b>45.90</b>	<b>61.70</b>	64.09	<b>31.40</b>	39.61	75.99	27.17	<b>53.78</b>	31.23	39.77	20.94	47.10	44.89	77.57%
ReplaceMe (LS)	37.5%	41.39	59.96	64.33	29.80	38.69	73.21	26.81	52.97	30.03	40.61	21.47	60.00	44.94	77.65%
ReplaceMe (Cosine)		45.09	61.32	62.19	29.60	<b>39.66</b>	67.49	<b>29.62</b>	25.35	<b>31.40</b>	40.95	<b>22.61</b>	68.70	43.67	75.45%
SUBFIT		43.09	60.56	64.25	30.60	39.51	74.37	<b>29.62</b>	36.00	30.72	<b>42.85</b>	22.35	<b>69.50</b>	<b>45.28</b>	<b>78.24%</b>
<b>Qwen3-4B-Instruct</b>	Dense	43.42	69.70	56.75	40.80	46.32	84.83	39.17	72.18	43.17	55.43	33.30	67.50	54.38	100.00%
Streamline (FFN)		25.45	51.69	<b>52.49</b>	<b>36.00</b>	34.03	37.83	22.77	22.92	<b>28.07</b>	29.12	19.40	23.60	31.95	58.75%
Streamline (Layer)		20.87	46.52	49.09	32.60	33.62	64.28	23.01	22.95	24.83	25.59	20.07	18.10	31.79	58.47%
ReplaceMe (LS)	37.5%	20.21	48.64	49.96	30.80	34.14	67.22	25.46	23.34	23.89	30.56	21.47	23.10	33.23	61.11%
ReplaceMe (Cosine)		23.81	50.98	52.25	30.00	33.06	46.42	24.72	24.01	26.54	32.41	18.79	30.60	32.80	60.31%
SUBFIT		<b>28.08</b>	<b>54.90</b>	51.70	32.00	<b>37.92</b>	<b>71.01</b>	<b>31.33</b>	<b>41.01</b>	26.19	<b>33.04</b>	<b>24.09</b>	<b>52.50</b>	<b>40.31</b>	<b>74.13%</b>
<b>Qwen2.5-7B-Instruct</b>	Dense	65.48	73.50	61.01	44.00	45.75	85.81	47.49	73.51	43.34	50.84	34.17	55.40	56.69	100.00%
Streamline (FFN)		41.98	64.85	52.09	35.00	38.43	44.89	30.11	25.26	27.73	38.09	25.53	51.10	39.59	69.83%
Streamline (Layer)		<b>45.17</b>	<b>67.03</b>	51.38	37.20	39.10	39.08	30.84	26.09	29.69	37.46	26.30	50.80	40.01	70.58%
ReplaceMe (LS)	37.5%	43.91	66.05	<b>53.67</b>	36.20	39.15	61.74	29.13	<b>28.17</b>	<b>31.06</b>	40.24	26.53	51.80	42.30	74.62%
ReplaceMe (Cosine)		44.31	66.76	50.83	<b>37.60</b>	<b>40.12</b>	62.11	27.05	27.54	30.20	<b>44.49</b>	<b>26.80</b>	<b>57.90</b>	<b>42.98</b>	<b>75.81%</b>
SUBFIT		41.50	66.97	52.49	37.20	39.51	<b>63.06</b>	<b>32.68</b>	25.41	30.46	40.61	24.02	55.00	42.41	74.81%
<b>DeepSeek-7B-chat</b>	Dense	70.56	77.64	74.90	44.80	50.46	83.98	37.21	50.90	41.55	62.63	27.54	78.40	58.38	100.00%
Streamline (FFN)		25.86	52.45	63.30	30.40	36.54	66.12	24.72	23.05	27.13	27.02	17.39	21.40	34.62	59.29%
Streamline (Layer)		38.66	58.43	64.25	<b>35.00</b>	38.54	63.73	23.87	23.00	<b>27.30</b>	34.89	20.74	29.00	38.12	65.29%
ReplaceMe (LS)	37.5%	38.24	66.27	51.93	30.40	40.23	61.65	<b>26.32</b>	25.05	24.23	40.49	22.91	56.90	40.39	69.18%
ReplaceMe (Cosine)		<b>42.50</b>	<b>67.79</b>	52.49	32.00	39.51	61.47	25.21	24.54	25.77	<b>44.11</b>	<b>23.82</b>	<b>61.10</b>	<b>41.69</b>	<b>71.41%</b>
SUBFIT		37.01	58.38	<b>65.51</b>	31.80	<b>40.58</b>	<b>71.62</b>	26.07	<b>29.75</b>	26.54	35.06	22.08	41.50	40.49	69.36%
<b>Llama-3.1-8B-Instruct</b>	Dense	72.52	79.49	77.82	49.00	50.20	83.88	40.39	68.79	53.58	75.76	26.80	91.70	64.16	100.00%
Streamline (FFN)		37.31	56.64	66.93	31.60	36.64	78.87	28.89	22.96	28.58	36.41	19.70	39.50	40.34	62.87%
Streamline (Layer)		42.96	60.45	69.06	<b>32.20</b>	38.95	80.03	30.35	45.24	31.40	<b>43.56</b>	19.97	58.20	46.03	71.74%
ReplaceMe (LS)	37.5%	40.07	58.65	67.64	30.60	39.41	<b>82.78</b>	31.33	<b>48.52</b>	30.46	41.33	21.27	58.10	45.85	71.46%
ReplaceMe (Cosine)		42.63	59.36	65.82	29.20	39.36	79.05	31.46	37.10	31.57	41.08	<b>22.35</b>	70.50	45.79	71.37%
SUBFIT		<b>47.54</b>	<b>62.57</b>	<b>70.24</b>	31.00	<b>41.50</b>	78.65	<b>32.80</b>	28.42	<b>33.11</b>	43.31	21.47	<b>72.60</b>	<b>46.94</b>	<b>73.15%</b>

Table A7: GSM8K accuracy (%) across instruction-tuned models and sparsity levels. Dense denotes the uncompressed model. Spread is the gap between the best and worst sparse methods for the same model and sparsity, highlighting GSM8K’s instability under compression.

Model	Sparsity	Dense	SL-FFN	SL-Layer	RM-LS	RM-Cos.	SUBFIT	Spread
<b>Llama-3.2-3B-Instruct</b>	Dense	67.7	–	–	–	–	–	–
	12.5%		32.1	<b>47.5</b>	40.8	40.9	2.3	45.3
	20%		2.6	<b>11.6</b>	9.1	8.5	2.7	9.0
	25%		3.5	3.8	<b>5.0</b>	3.2	1.1	3.9
	30%		2.0	2.4	<b>2.9</b>	2.1	1.8	1.1
	37.5%		1.7	1.9	2.0	<b>2.4</b>	2.1	0.6
<b>Qwen3-4B-Instruct</b>	Dense	84.0	–	–	–	–	–	–
	12.5%		38.5	31.7	12.7	39.7	<b>60.7</b>	48.0
	20%		4.0	2.5	2.3	5.6	<b>22.0</b>	19.7
	25%		2.0	0.5	2.0	1.7	<b>2.9</b>	2.4
	30%		0.1	0.0	1.8	<b>2.3</b>	2.2	2.3
	37.5%		0.0	0.0	1.1	0.5	<b>1.4</b>	1.4
<b>Qwen2.5-7B-Instruct</b>	Dense	81.2	–	–	–	–	–	–
	12.5%		7.3	16.1	<b>31.9</b>	30.0	24.1	24.6
	20%		2.0	4.1	6.3	4.5	<b>7.1</b>	5.1
	25%		1.8	1.7	2.4	2.6	<b>3.6</b>	1.8
	30%		1.5	1.4	2.5	<b>2.6</b>	1.6	1.2
	37.5%		1.8	1.3	1.5	<b>2.2</b>	1.4	0.9
<b>DeepSeek-7B-chat</b>	Dense	51.0	–	–	–	–	–	–
	12.5%		24.6	23.1	24.2	22.0	<b>25.4</b>	3.4
	20%		3.3	9.5	9.7	5.2	<b>12.8</b>	9.5
	25%		1.6	2.0	2.0	2.3	<b>3.6</b>	2.0
	30%		0.2	1.1	1.7	1.4	<b>3.3</b>	3.1
	37.5%		0.0	0.5	1.3	<b>2.2</b>	1.7	2.2
<b>Llama-3.1-8B-Instruct</b>	Dense	79.2	–	–	–	–	–	–
	12.5%		62.1	62.3	<b>65.5</b>	65.3	56.3	9.2
	20%		39.7	31.6	40.6	<b>52.8</b>	30.6	22.2
	25%		4.0	3.6	10.5	<b>16.7</b>	8.3	13.1
	30%		1.7	1.4	<b>2.7</b>	2.6	1.8	1.2
	37.5%		1.5	1.7	1.7	<b>2.0</b>	2.0	0.5

singular components of the original layer weights, rather than fitting a new residual map from cali-

bration activations for each removed Attention or FeedForward submodule. Lastly, ELM replaces

Table A8: Average pruning runtime in seconds across models for base PPL and instruct downstream experiments.

Method	Base PPL runtime (s) ↓					Instruct runtime (s) ↓				
	12.5%	20%	25%	30%	37.5%	12.5%	20%	25%	30%	37.5%
Streamline (FFN)	764	<b>766</b>	912	740	720	<b>405</b>	472	<b>429</b>	<b>390</b>	<b>367</b>
Streamline (Layer)	<b>683</b>	1224	<b>612</b>	<b>723</b>	<b>597</b>	484	<b>431</b>	523	407	422
ReplaceMe (LS)	1273	1342	1141	1333	1160	1012	1021	1206	1015	1013
ReplaceMe (Cosine)	1662	1631	1808	1643	1624	2672	2734	2692	2604	2659
SUBFIT	1905	2436	2231	2673	2410	2028	2100	2137	2155	2550

groups of Transformer layers with fixed-point modules selected by a learned policy and adapted with task-specific LoRA fine-tuning, whereas our setting is post-training and calibration-only. We therefore use Streamline and ReplaceMe as the main experimental comparisons, and discuss these other methods as related recovery approaches rather than direct baselines.

We also did not include any *structured pruning* algorithm such as SliceGPT (Ashkboos et al., 2024), LLM-Pruner (Ma et al., 2023), Laco (Yang et al., 2024), UIDL (Gromov et al., 2025) since the replacement-based compression literature has already shown to achieve better performance compared to standard structured pruning in (Chen et al., 2025b; Shopkhoev et al., 2025). This is also supported by our results in Table 5.

**Calibration.** All methods use the same calibration corpus and budget. For base models, we use SlimPajama (Shen et al., 2023); for instruction-tuned models, we use SlimOrca (Mukherjee et al., 2023). In both cases, we sample 8k sequences at maximum length 1024 tokens, yielding approximately 8M calibration tokens per fit. No calibration data overlaps with any evaluation benchmark.

**SUBFIT hyperparameters.** For SUBFIT, we use attention bypass rank  $r = 256$  and FFN shared-basis rank  $r = 4096$ ; both ranks were selected based on the rank-sensitivity ablation (Section 5). The ridge regularization in the closed-form fit Eq. (5) is set to  $\lambda = 10^{-6}$ ; the small constant in the impact score in Eq. (1) is  $\epsilon = 10^{-6}$ .

**Hardware and runtime.** All inference and calibration experiments are run on a single NVIDIA A100 80GB GPU. Compression of one model-sparsity configuration takes between approximately 2,000 and 2,600 seconds, comparable to ReplaceMe (Cosine) and slower than Streamline; this cost is paid once at compression time and does not affect deployed latency. Inference benchmarks (TTFT and decode speedup in Table 4) are also run on the same A100 80GB hardware.

**Reproducibility.** All compression and evaluation

runs use a fixed random seed for calibration sampling and token-level sub-sampling. Source code, replication scripts, and the full set of per-model compressed checkpoints will be made available after the review.

## D Limitations and Additional Analysis

SUBFIT introduces explicit bypass parameters for selected Attention and FFN submodules. Table A10 summarizes the deployed parameters and MAC overhead. Added parameters remain around 10% of the removed parameters, while added MACs are around 15% of the removed MACs. This cost is the price of fitting explicit residual compensation modules; in contrast, ReplaceMe variants add no deployed parameters because their transformations are folded into existing weights.

Model	Sparsity	Method	Removed (M)	Added (M)	Add/Remove ↓	Added Attn. (M)	Added FNN (M)
Llama-3.2-3B	12.5%	Streamline (FFN)	402.7	75.5	18.7%	0.0	75.5
		Streamline (Layer)	402.7	100.7	25.0%	25.2	75.5
		ReplaceMe (LS)	402.7	0.0	0.0%	0.0	0.0
		ReplaceMe (Cosine)	402.7	0.0	0.0%	0.0	0.0
		SUBFIT	402.7	53.6	13.3%	6.3	47.2
	25%	Streamline (FFN)	704.7	75.5	10.7%	0.0	75.5
		Streamline (Layer)	704.7	100.7	14.3%	25.2	75.5
		ReplaceMe (LS)	704.7	0.0	0.0%	0.0	0.0
		ReplaceMe (Cosine)	704.7	0.0	0.0%	0.0	0.0
		SUBFIT	704.7	86.6	12.3%	11.1	75.6
	37.5%	Streamline (FFN)	1006.7	75.5	7.5%	0.0	75.5
		Streamline (Layer)	1006.7	100.7	10.0%	25.2	75.5
		ReplaceMe (LS)	1006.7	0.0	0.0%	0.0	0.0
		ReplaceMe (Cosine)	1006.7	0.0	0.0%	0.0	0.0
		SUBFIT	1006.7	119.7	11.9%	15.8	103.9
Qwen3-4B	12.5%	Streamline (FFN)	403.7	74.7	18.5%	0.0	74.7
		Streamline (Layer)	403.7	100.9	25.0%	26.2	74.7
		ReplaceMe (LS)	403.7	0.0	0.0%	0.0	0.0
		ReplaceMe (Cosine)	403.7	0.0	0.0%	0.0	0.0
		SUBFIT	403.7	38.1	9.4%	5.3	32.8
	25%	Streamline (FFN)	908.4	74.7	8.2%	0.0	74.7
		Streamline (Layer)	908.4	100.9	11.1%	26.2	74.7
		ReplaceMe (LS)	908.4	0.0	0.0%	0.0	0.0
		ReplaceMe (Cosine)	908.4	0.0	0.0%	0.0	0.0
		SUBFIT	908.4	77.5	8.5%	11.9	65.6
	37.5%	Streamline (FFN)	1413.0	74.7	5.3%	0.0	74.7
		Streamline (Layer)	1413.0	100.9	7.1%	26.2	74.7
		ReplaceMe (LS)	1413.0	0.0	0.0%	0.0	0.0
		ReplaceMe (Cosine)	1413.0	0.0	0.0%	0.0	0.0
		SUBFIT	1413.0	116.9	8.3%	18.5	98.4
DeepSeek-7B	12.5%	Streamline (FFN)	809.5	135.3	16.7%	0.0	135.3
		Streamline (Layer)	809.5	202.4	25.0%	67.1	135.3
		ReplaceMe (LS)	809.5	0.0	0.0%	0.0	0.0
		ReplaceMe (Cosine)	809.5	0.0	0.0%	0.0	0.0
		SUBFIT	809.5	92.4	11.4%	8.4	83.9
	25%	Streamline (FFN)	1619.1	135.3	8.4%	0.0	135.3
		Streamline (Layer)	1619.1	202.4	12.5%	67.1	135.3
		ReplaceMe (LS)	1619.1	0.0	0.0%	0.0	0.0
		ReplaceMe (Cosine)	1619.1	0.0	0.0%	0.0	0.0
		SUBFIT	1619.1	168.0	10.4%	16.9	151.1
	37.5%	Streamline (FFN)	2226.2	135.3	6.1%	0.0	135.3
		Streamline (Layer)	2226.2	202.4	9.1%	67.1	135.3
		ReplaceMe (LS)	2226.2	0.0	0.0%	0.0	0.0
		ReplaceMe (Cosine)	2226.2	0.0	0.0%	0.0	0.0
		SUBFIT	2226.2	224.7	10.1%	23.2	201.5
Llama-3.1-8B	12.5%	Streamline (FFN)	872.4	176.2	20.2%	0.0	176.2
		Streamline (Layer)	872.4	218.1	25.0%	41.9	176.2
		ReplaceMe (LS)	872.4	0.0	0.0%	0.0	0.0
		ReplaceMe (Cosine)	872.4	0.0	0.0%	0.0	0.0
		SUBFIT	872.4	92.4	10.6%	8.4	83.9
	25%	Streamline (FFN)	1744.9	176.2	10.1%	0.0	176.2
		Streamline (Layer)	1744.9	218.1	12.5%	41.9	176.2
		ReplaceMe (LS)	1744.9	0.0	0.0%	0.0	0.0
		ReplaceMe (Cosine)	1744.9	0.0	0.0%	0.0	0.0
		SUBFIT	1744.9	168.0	9.6%	16.9	151.1
	37.5%	Streamline (FFN)	2617.3	176.2	6.7%	0.0	176.2
		Streamline (Layer)	2617.3	218.1	8.3%	41.9	176.2
		ReplaceMe (LS)	2617.3	0.0	0.0%	0.0	0.0
		ReplaceMe (Cosine)	2617.3	0.0	0.0%	0.0	0.0
		SUBFIT	2617.3	243.6	9.3%	25.3	218.3
Qwen3-8B	12.5%	Streamline (FFN)	771.8	151.0	19.6%	0.0	151.0
		Streamline (Layer)	771.8	192.9	25.0%	41.9	151.0
		ReplaceMe (LS)	771.8	0.0	0.0%	0.0	0.0
		ReplaceMe (Cosine)	771.8	0.0	0.0%	0.0	0.0
		SUBFIT	771.8	92.4	12.0%	8.4	83.9
	25%	Streamline (FFN)	1736.5	151.0	8.7%	0.0	151.0
		Streamline (Layer)	1736.5	192.9	11.1%	41.9	151.0
		ReplaceMe (LS)	1736.5	0.0	0.0%	0.0	0.0
		ReplaceMe (Cosine)	1736.5	0.0	0.0%	0.0	0.0
		SUBFIT	1736.5	186.9	10.8%	19.0	167.9
	37.5%	Streamline (FFN)	2701.2	151.0	5.6%	0.0	151.0
		Streamline (Layer)	2701.2	192.9	7.1%	41.9	151.0
		ReplaceMe (LS)	2701.2	0.0	0.0%	0.0	0.0
		ReplaceMe (Cosine)	2701.2	0.0	0.0%	0.0	0.0
		SUBFIT	2701.2	281.4	10.4%	29.5	251.8

Table A9: Removed parameters, deployed added compensation parameters, and added/removed ratio for base models. For SUBFIT, the table reports the Attention and FFN compensation breakdown; the FFN replacement uses a shared basis counted once per model. Streamline FFN removes the same decoder-layer budget as the other depth-replacement methods but deploys an FFN-only replacement. ReplaceMe folds its fitted full-rank transform into an existing FeedForward projection, so it adds no deployed parameters.

Table A10: Theoretical MACs removed and added for one forward pass with sequence length 2048. Attention MACs include QKV/O projections plus QK and AV products; FeedForward MACs include the three FeedForward projections. For SUBFIT, added MACs are split into Attention and FeedForward residual compensation.

Sparsity	Method	Removed (GMACs)	Added (GMACs)	Add/Remove ↓	Added attn	Added FeedForward
<b>Base models</b>						
12.5%	Streamline (FFN)	1003.7	250.9	25.0%	0.0	250.9
	Streamline (Layer)	1465.9	366.5	25.0%	115.5	250.9
	ReplaceMe (LS)	1465.9	0.0	0.0%	0.0	0.0
	ReplaceMe (Cosine)	1465.9	0.0	0.0%	0.0	0.0
	SUBFIT	1465.9	232.4	15.8%	15.1	217.4
25%	Streamline (FFN)	2069.0	250.9	12.3%	0.0	250.9
	Streamline (Layer)	3019.5	366.5	12.3%	115.5	250.9
	ReplaceMe (LS)	3019.5	0.0	0.0%	0.0	0.0
	ReplaceMe (Cosine)	3019.5	0.0	0.0%	0.0	0.0
	SUBFIT	3019.5	477.0	15.8%	30.9	446.1
37.5%	Streamline (FFN)	3078.8	250.9	8.3%	0.0	250.9
	Streamline (Layer)	4483.3	366.5	8.3%	115.5	250.9
	ReplaceMe (LS)	4483.3	0.0	0.0%	0.0	0.0
	ReplaceMe (Cosine)	4483.3	0.0	0.0%	0.0	0.0
	SUBFIT	4483.3	706.9	15.8%	45.8	661.1
<b>Instruct models</b>						
12.5%	Streamline (FFN)	1090.1	272.5	25.0%	0.0	272.5
	Streamline (Layer)	1528.1	382.0	25.0%	109.5	272.5
	ReplaceMe (LS)	1528.1	0.0	0.0%	0.0	0.0
	ReplaceMe (Cosine)	1528.1	0.0	0.0%	0.0	0.0
	SUBFIT	1528.1	219.1	14.6%	14.6	204.5
25%	Streamline (FFN)	2096.4	272.5	12.9%	0.0	272.5
	Streamline (Layer)	2956.7	382.0	12.9%	109.5	272.5
	ReplaceMe (LS)	2956.7	0.0	0.0%	0.0	0.0
	ReplaceMe (Cosine)	2956.7	0.0	0.0%	0.0	0.0
	SUBFIT	2956.7	424.5	14.6%	28.4	396.1
37.5%	Streamline (FFN)	3047.3	272.5	8.9%	0.0	272.5
	Streamline (Layer)	4295.4	382.0	8.9%	109.5	272.5
	ReplaceMe (LS)	4295.4	0.0	0.0%	0.0	0.0
	ReplaceMe (Cosine)	4295.4	0.0	0.0%	0.0	0.0
	SUBFIT	4295.4	615.2	14.6%	41.3	573.9